THE DEVELOPMENT AND ANALYSIS OF A HEATERLESS, INSERTLESS, MICROPLASMA-BASED HOLLOW CATHODE

By

RYAN P. GOTT

A THESIS

Submitted in partial fulfillment of the requirements
for the degree of Master of Science in Engineering
in
The Department of Mechanical and Aerospace Engineering
to
The School of Graduate Studies
of
The University of Alabama in Huntsville

HUNTSVILLE, ALABAMA

2017

In presenting this thesis in partial fulfillment of the requirements for a master's degree from The University of Alabama in Huntsville, I agree that the library of this University shall make it freely available for inspection. I further agree that permission for extensive copying for scholarly purposes may be granted by my advisor or, in his/her absence, by the Chair of the Department or the Dean of the School of Graduate Studies. It is also understood that due recognition shall be given to me and to The University of Alabama in Huntsville in any scholarly use which may be made of any material in this thesis.

_____ _____

Ryan P. Gott Date

THESIS APPROVAL FORM

Submitted by Ryan P. Gott in partial fulfillment of the requirements for the degree of Master of Science in Engineering in Aerospace Systems Engineering and accepted on behalf of the Faculty of the School of Graduate Studies by the thesis committee.

We, the undersigned members of the Graduate Faculty of The University of Alabama in Huntsville, certify that we have advised and/or supervised the candidate of the work described in this thesis. We further certify that we have reviewed the thesis manuscript and approve it in partial fulfillment of the requirements for the degree of Master of Science in Engineering in Aerospace Systems Engineering.

_____ Committee Chair
Dr. Kunning Xu Date

_____
Dr. Brian Landrum Date

_____
Dr. Jason Cassibry Date

_____ Department Chair
Dr. Keith Hollingsworth Date

_____ College Dean
Dr. Shankar Mahalingam Date

_____ Graduate Dean
Dr. David Berkowitz Date

ABSTRACT

The School of Graduate Studies
The University of Alabama in Huntsville

Degree Master of Science in Engineering
College/Dept. Engineering/Mechanical and Aerospace Engineering
Name of Candidate Ryan P. Gott
Title The Development and Analysis of a Heaterless, Insertless, Microplasma-Based Cathode

Hall Effect Thrusters and Ion Thrusters use the expulsion of positively charged ions to generate a thrust force. In order to generate those ions and to prevent the ion exhaust from negatively charging the thrusters, a source of free electrons is needed. Hollow cathodes are commonly used as the electron source, due to their high electron density and current. However, the power required for most hollow cathodes is still too high for small satellites. The component that draws the largest amount of power is the heater. A heater is necessary to excite the thermionic insert to its emission temperature. Heaterless cathodes have been studied previously, but still required an insert material with a relatively low breakdown voltage. Insert materials, such as Barium Oxide (BaO) and Lanthanum Hexaboride (LaB_6), have high rates of deterioration and thus limit the life of the cathode. The contamination caused by the emissive materials also causes erosion and deterioration of the cathode. In this research, a heaterless, insertless hollow cathode was developed by using an argon microplasma generated in a quartz tube with a tungsten filament and brass ion collector. The cathode produced 150 milliamps of current at an anode voltage of 300 V with an input power of 75 W. Various power sources, configurations, and flow rates have been analyzed and tested. Performance of the cathode was characterized using Langmuir Probes, numerical models, and direct current measurement.

Abstract Approval: Committee Chair _____
Dr. Kunning Xu

Department Chair _____
Dr. Keith Hollingsworth

Graduate Dean _____
Dr. David Berkowitz

ACKNOWLEDGEMENTS

I would like to thank my advisor, Dr. Gabe Xu, for giving me the opportunity to pursue research in the Plasma and Electrodynamics Research Lab at the Propulsion Research Center. Without his continual support and guidance, this work would not have been possible. As one of his students, I have not only become a better engineer, but also a better researcher.

I would also like to thank the Propulsion Research Center Lab Supervisor Dr. David Lineberry and Facility Engineer Tony Hall, who were always willing to answer any question I had. Their feedback on experimental setups, analysis, and safety were vital for the success of this work.

Credit is also due to my fellow colleagues at the Plasma and Electrodynamics Research Lab. I am grateful for the assistance of Steven Doyle, Roberto Dextre, Paulo Salvador, Ethan Hopping, TJ Miller, Natalie Mann, and Noah Latham with experimental setup and testing.

I would like to thank my girlfriend, Amanda Falkner, for putting up with me through this process and continually supporting my dreams. Thank you for helping me practice presentations, listening to me talk about the most boring parts of my research, and cheering me on during the hardest days.

Finally, I would like to thank my siblings, Andrew and Lauren GottWorth and Emily and Jason White, and my parents, Tim and Ellen Gott for their continuous love and support. I have made it to this point in my life because of the love you all have given me, and I am forever grateful.

TABLE OF CONTENTS

LIST OF FIGURES

LIST OF TABLES

LIST OF SYMBOLS

A	Emission constant
A_{eff}	Effective plasma surface area
$A_{i,e}$	Ion and electron loss areas
A_p	Langmuir probe surface area
A_t	Tube exit area
d	Tube diameter
e	Electron charge
ε_0	Permittivity of free space
$\varepsilon_{T,c}$	Energy loss
ζ	Viscosity
Γ	Current flux
F	Thrust
g_0	Earth gravity
$h_{l,R}$	Plasma edge-to-center ratios
I	Current
i_n	Saturation current
J	Current density
k	Boltzmann's constant
λ_D	Debye length
λ_i	Mean-free-path
l	Plasma length
M	Mass of Argon

$\dot{m}$	Mass flow rate
$n_{e,i,0}$	Electron, ion, and neutral density
P	Operating pressure
P_{abs}	Absorbed power
Q	Flow rate
q	Charge
R	Plasma radius
T_e	Electron temperature
T_g	Gas temperature
T_r	Temperature ratio
u_B	Bohm velocity
v_e	Exit velocity

I seem to have been only like a boy playing on the seashore, and diverting myself in now and then finding a smoother pebble or a prettier shell than ordinary, whilst the great ocean of truth lay all undiscovered before me.
- Isaac Newton

Chapter 1

INTRODUCTION

A simple intuition, a single observation, can open vistas of unimagined potential. Once caught in the web of an idea, the researcher is happily doomed, for the outcome is always uncertain, and the resolution of the mystery may take years to unfold.

- Wade Davis

There are two predominant types of in-space propulsion systems for satellites and spacecraft: chemical and electrical. While chemical propulsion devices can provide higher thrust, which is necessary for planetary launch and fast maneuvers, electric propulsion (EP) provides a more efficient, though slower, alternative for orbital maneuvers and positioning. A key efficiency parameter in propulsion is the specific impulse (Isp). Isp is akin to a mile-per-gallon metric that is defined by thrust (F), mass flow rate ($\dot{m}$), Earth gravity (g_0), and exit velocity (v_e) as shown in Equation 1.1.

$$Isp = \frac{F}{\dot{m} g_0} = \frac{v_e}{g_0} \tag{1.1}$$

As the equation shows, a higher exit velocity produces better Isp. EP provides an alternative to chemical methods that maximizes Isp by using low mass flow rates and producing high exit velocities. Hall thrusters and ion engines are two EP devices that can

produce high Isp. While chemical propulsion devices can produce a wide range of thrusts from 1 N to 10,000 kN with Isp ranging from 100-450 s, EP devices can provide only up to 5 N of thrust but with Isp ranging from 1000-8000 s.[1]

A new and fast growing area where EP thrusters could be useful is on small satellites. Small satellites are a fast growing industry because they are low cost and can provide similar capabilities as large multi-million dollar satellites. They can provide low-cost space access for many applications, such as communication, defense, and research. Today, small satellites do not have onboard propulsion due to size and power limitation and launch regulations. This means small satellites in lower orbits have a limited lifetime due to atmospheric drag, which will cause them to deorbit and burn up during reentry into Earth's atmosphere.[2] A propulsion system can greatly benefit small satellite missions by enabling orbit maneuvers and longer orbit lifetimes. EP is especially attractive for small satellites due to their high Isp.[3] CubeSats, for example, need numerous small, efficient pulses for guidance and navigation, thus a low thrust, high efficiency propulsion system such as EP is more attractive given the limit mass of these satellites.

One obstacle for EP use on small satellites is the power requirements to operate these thrusters. One of the biggest power consumers on EP thrusters such as Ion and Hall Thrusters are the cathodes that provide free electrons for ionization and neutralization. Cathodes are used as an electron source in a variety of applications, ranging from medical[4] to propulsion[5]. They can be as simple as a single wire, or can be complicated with a heater, multiple circuits, and multiple power sources. Ion engines and Hall thrusters require an electron source for ionization and beam neutralization that can efficiently provide electrons for thousands of hours. Several types of cathodes have been developed for these electric

propulsion devices such as hollow cathodes, Radio Frequency (RF) cathodes, and bulk emitter cathodes.[5–7]

Hollow cathodes have been the most common cathodes used for EP because they can generate high currents up to 250 A with relatively low power input.[8] However, developments are needed to reduce power requirements even further for use on small satellites. In most hollow cathodes, the heater draws the most power, requiring up to 300 W in some cases.[8] The heater is used in these devices to heat a thermionic insert to emission temperature, but an insertless design could remove the need for the heater altogether.

One way to create an insertless design is by using a microplasma jet. Microplasmas are small scale ionized discharges, typically millimeters or smaller in size, that can produce high electron densities (up to 10^{16} cm^{-1}).[9] At atmospheric pressures, microplasmas can operate stably without arcing. This allows for medical and biological applications.[10] However, the high density plasma can also be generated at vacuum pressures, allowing for potential use of this technology as a hollow cathode. Thus this research seeks to study if microplasma jets can be adapted as a low-power cathode electron source for EP devices.

1.1 Problem Statement

Traditional hollow cathodes require high power levels and long start-up times, which make these cathodes unsuitable for small satellites. Developing cathode technology that does not require a heater could reduce the power requirements, which would allow for the use of EP systems on small satellites. The main function of the heater is to heat a thermionic material which creates the cathode plasma for electron extraction. If the cathode plasma is generated directly with a low power method, the insert and the associated heater can be

removed. A target small satellite cathode should be able to provide over 100 mA of output current with an input power around 10 W and a startup time on the order of 10s of seconds. Previously, Xu and Doyle[10] studied an atmospheric microplasma jet (AMPJ) that could generate a small plasma with pulsed dc power with relatively low powers. The question thus arose whether this microplasma could be adapted for use as a cathode to extract electrons. Additionally, the AMPJ was built from inert materials such as quartz and tungsten, meaning it may be compatible with new propellants being investigated for EP such as iodine and sulfur. The research presented in this thesis aimed to characterize the behavior of the microplasma in a vacuum environment for the purpose of electron extraction as a cathode. The end goal is to optimize this microplasma cathode to achieve a low power design suitable for small satellites.

This cathode was experimentally tested to determine the plasma and electron extraction over the operating range. Langmuir probes were used to measure electron temperature and density in the plasma plume. Electron temperature and density were used to compare modes of operation using an analytical model to calculate theoretical current. Direct current measurements using an anode were also made and compared to this theoretical model. Comparisons were made between ac or pulsed dc power, argon flow rate, pulse width, frequency, and voltage. Experiments were then made to find a suitable operating condition for the cathode.

1.2 Research Contributions

The objective of the research was to modify a microplasma jet to develop a heaterless, insertless, hollow cathode in order to provide a suitable neutralizing source for small satellites. Multiple operating regimes were explored and analyzed to study the performance of the cathode. By furthering the knowledge of the operating regimes, steps were made toward creating an efficient, low power hollow cathode. These developments also aid in the overall goal of providing low-cost, efficient propulsion on small satellites.

Chapter 2

BACKGROUND

There is not a discovery in science, however revolutionary, however sparkling with insight, that does not arise out of what went before. – Isaac Asimov

Ion and Hall thrusters are EP devices that use beams of accelerated positive ions to generate thrust. This means that electrons, or negative ions, must be introduced into the ion beam as it leaves the thruster to prevent the spacecraft from charging negatively and attracting the emitted positive ion beam. These neutralization electrons are typically provided by cathodes, which also serve to provide electrons to generate the plasma in the thruster via electron impact ionization. Cathodes technologies are diverse and plentiful, but only a few are commonly used in space applications. In normal usage, the term cathode is defined as a negatively charged electrode. In EP, the cathode is often also a source of free electrons. These cathodes can be as simple as a single wire or as complex as a device with propellant, electrodes, and multiple power sources. For example, one of the simplest cathodes is just a tungsten filament with a current running through it, similar to an incandescence light bulb. They are placed at the exit of thrusters or other ion sources to neutralize the beam. Filament cathodes have too many limitations for space applications,

such as short lifetimes (200-300 hours) and limited performance. The short lifetimes are due to issues such as sputter erosion, evaporation of the tungsten, and the high temperatures needed to achieve emission.[1]

Another simple cathode is the single crystal emitter, most commonly used in electron microscopes.[11] This type of cathode usually uses lanthanum hexaboride (LaB_6)[5] or cesium hexaboride (CeB_6)[12] as the emission material. These compounds both have low work functions (2.4-2.8 eV) and low evaporation rates. These cathodes operate by heating the LaB_6 or CeB_6 crystal ohmically. Once these materials reach their emission temperatures, electrons are emitted from the surface. This process only requires 10-20 W of power, but produces very low currents (10s of mA).[12]

Other cathode designs have been developed for specific applications. For example, Carbon Nanotube (CNT) cathode neutralizers have been used on colloid thrusters and x-ray spectrometers.[13,3,14] CNT devices produce μA of current for electrospray using less than 0.5 W. The device accelerates the electrons to cause rapid, high velocity collisions that emit x-rays. However, larger current outputs (on the order of mA to A) are needed for most EP devices.

While these cathodes are simple, they are not very efficient. Most thrusters need high current to power ratios. Traditionally, hollow cathodes have been used as electron sources for ion and Hall thrusters because of their high electron current density. A plethora of designs have been used for hollow cathodes, with the majority including a heater, orifice plate, and an insert material. Hollow cathodes use heating coils or filaments to bring a thermionic insert material to its emission temperature. Once the insert reaches its emission temperature, electrons are released from the surface of the material. Then, the propellant

gas, for example argon or xenon, is flowed into the insert region. The emitted electrons collide and ionize the gas to produce a plasma. Electrons from this plasma are extracted through the orifice by a positively biased electrode, known as the keeper to generate a high electron current.[1] The keeper also serves to turn the discharge on, maintain temperature, and protect the cathode from ion bombardment.

One of the most common inserts is barium oxide (BaO) impregnated tungsten. Due to tungsten's high work function, various oxides were tested to lower the heat power required to reach the emission temperature. The BaO mix was found to be the most effective, and was adopted as the best insert material.[15] A comparison of different insert materials is shown in Figure 2.1.

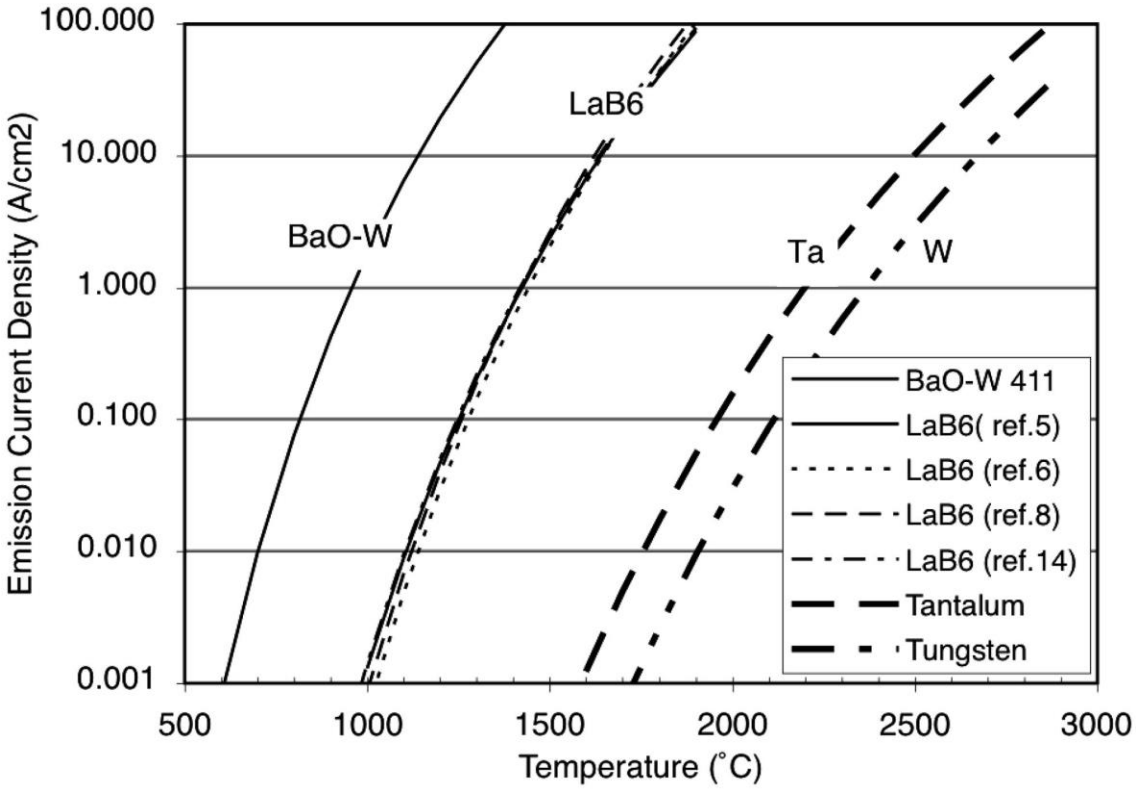

Figure 2.1. Differences in emission currents for various insert materials.[5]

BaO hollow cathodes were the most commonly used cathode in the US for half a century because they can produce high currents and have the potential to operate for 10 million hours.[16] However, the susceptibility of the BaO material to impurities such as water and oxygen can cause their performance to decline after just hundreds of hours due to insert deterioration, contamination, and barium diffusion rates rendering them less suitable for sustained use.[17] This has led to numerous alternative designs.

More recently, LaB_6 hollow cathodes have become more common, especially in research labs. These cathodes replace the BaO insert with a LaB_6 bulk emitter. Unlike the single crystal devices used before, LaB_6 cathodes use a full LaB_6 insert as the basis for the cathode. LaB_6 has a higher work function than BaO (2.67 eV compared to 2.06 eV), but are more resistant to poisoning and degradation and therefore can provide a longer lifetime than the BaO cathodes.[1,5] Other recent designs have moved towards heaterless and/or insertless designs. Radio Frequency (RF) cathodes are one common variation that use RF waves to ionize a gas and produce electrons.[18] Other designs have used self-heating methods to increase the temperature without using a heater. These designs can cut down on input power and startup time compared to traditional hollow cathodes, but improvements are needed to further reduce power input for use on small satellites.

2.1 Power Requirements

High-powered Hall thrusters need 20-100 kW, which requires 50-400 A from the hollow cathodes. New, larger EP devices need to process 100-200 kW of power, meaning they will need 330-660 A of discharge current, with lifetimes as high as 100 kh.[19] However, small spacecraft are power limited as well, meaning that the discharge current must be

produced with minimal power usage. Because of this, devices with low electron extraction costs are desired. Electron extraction costs can vary dramatically between devices, ranging as high as 4000 W/A for a CNT cathode [20] to as low as 33 W/A for a BaO hollow cathode.[6]

On the other hand, small satellites are more dramatically power limited, but require much lower extraction currents. For a 1U CubeSat, the maximum power budget is only 1-2.5 W.[21] This increases to 2-5 W for a 2U, and 7 to 20 W for a 3U.[22,23] NASA has recently looked into 6U and 12 U iSAT missions that will utilize a 200 W Hall Thruster.[24] This will require a lower extraction current, on the order of 500 mA. Additionally, in traditional hollow cathodes, the side of the insert, heater, and thus cathode scales with the maximum discharge current. This causes issues for thrusters and devices that are geometrically constrained, such as CubeSats or internally-mounted cathodes for Hall Thrusters.[25,26] For these devices, a small cathode is needed that uses around 10 W of power to produce 0.5-1 A of discharge current.

2.2 Hollow Cathodes

Hollow cathodes are a type of electron source that produces high electron current density. While most of these devices use thermionic insert materials to produce electrons, they are very diverse in design and performance. The general design is shown in Figure 2.2.

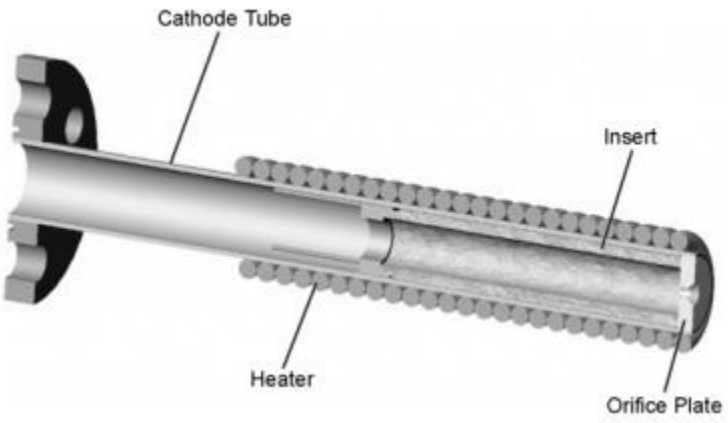

Figure 2.2. A typical hollow cathode.[16]

For cathodes in general, the amount of electron current extracted is equal to the electron flux and limited by the plasma density, the neutral gas flow rate, and the ion loss area of the source.[17] In order to maintain quasi-neutrality in the cathode plasma, the electron flux must balance the ion flux. Therefore, the ratio between these two must be balanced by the ratio of the ion and electron loss areas. This relationship is demonstrated in Equation 2.1,

$$\Gamma_e = \Gamma_i \frac{A_i}{A_e} \tag{2.1}$$

where Γ is flux, A is loss area, and the i and e subscripts refer to ions and electrons respectively. This equation is used to determine the size of the ion and electron loss areas in most designs. The initial electron source in hollow cathodes is the thermionic insert material which emits electrons once heated. These insert materials are key to operation of conventional hollow cathode, and thus one of the main lifetime limiters.

2.3 Insert Materials

Electron emission behavior in hollow cathode inserts can be described by the Richardson-Duschman equation, as shown in Equation 2.2,[1]

$$J = AT^2 e^{\frac{-q\varphi}{kT}} \tag{2.2}$$

where J is current density, A is the emission constant, k is Boltzmann's constant, T is temperature, ϕ is work function, and q is the elementary charge. The work function is a property of the insert material in the cathode that describes how much energy is needed to emit electrons, and is an important factor in the development of hollow cathodes. A lower work function means that lower temperatures are required to sustain a given current density. For example, BaO has a work function of 2.06 eV, and requires a temperature of 1000 ^{o}C to reach an emission density of 20 A/cm^2. LaB_6, on the other hand, has a work function of 2.67 eV, and requires a temperature of 1650 ^{o}C to reach the same emission density. Because propulsion devices are limited by the melting temperature of the materials and the power limitations of the system, a considerable amount of work has been done to reduce the work functions of insert materials.

There are two commonly used types of high current density hollow cathodes: dispenser and bulk emitter. The most common dispenser cathode is a “Type S”, or Barium Oxide (BaO) cathode, which uses a barium calcium aluminate impregnated tungsten insert with a work function of 2.06 eV.[16] Whereas dispenser cathodes use a bulk material doped with a low work function species, tungsten with BaO, to reduce the work function of the bulk material, bulk emitter cathodes use solely the solid bulk material itself. LaB_6 is the most common bulk emitter material. The LaB_6 cathodes are less reactive to propellant impurities, but require a high amount of heat energy with a work function of 2.67 eV.

2.4 Dispenser Hollow Cathodes

Dispenser cathodes operate by causing a chemical reaction within the material that make it easier to release electrons. When the insert is heated, the gaseous barium rises to the surface and lowers the work function.[27] Unfortunately, this means that the BaO materials require clean surfaces and are thus highly dependent on high purity environments. The presence of oxygen and water in the air or propellant can poison the insert and dramatically increase the work function. For this reason, ultra-high purity gases, 99.9995%, are typically used in BaO cathodes. These cathodes also must be stored in an inert atmosphere when not in vacuum, such as a nitrogen purge box. However, in the absence of impurities, dispenser cathodes have lower work functions than bulk emitters and are therefore preferred.

Since the 1960s, NASA has used primarily dispenser cathodes in Ion and Hall Thrusters. The most commonly used design was the BaO impregnated Philips cathode, designed by the U.S. Philips Corporation.[28] Levi determined that this design solved many thermal issues of previous cathodes and the chemical mixture effectively lowered the work function.[7] Various other chemical combinations were tested until the barium calcium aluminate impregnated tungsten design was discovered, and that design is still used today. A full summary of these chemical combinations is provided by Cronin.[15]

2.5 Bulk Emitter Hollow Cathodes

Unlike the BaO cathodes, LaB_6 does not require a chemical reaction and will emit electrons when it reaches high temperatures (1650 ^{o}C). Its work function of 2.67 eV is

higher than that of BaO dispenser cathodes (2.06 eV), which causes the need for a higher emission temperature than that of BaO (1000 ^{o}C), but it does not experience the same degradation. The BaO cathodes require ultra-pure propellant gas to prevent "poisoning" of the cathode.[5] While the emission temperature for LaB_6 is higher than dispenser cathodes, LaB_6 has shown longer lifetimes due to lower evaporation rates and less sensitivity to poisoning. However, these devices still experience erosion from the high energy ions. The overall performance of these devices is favorable compared to other hollow cathodes. Goebel and Chu found that LaB_6 can achieve higher current densities above 20 A/cm^2, and can produce 300 A of current for 10-20 kh of life.[8]

CeB_6 cathodes are very similar to LaB_6. The CeB_6 insert is also resistant to poisoning and even has a lower evaporation rate and work function (2.5 eV) than LaB_6. However, Warner found that CeB_6 had a lower emissivity and did not provide a significant improvement in performance compared to LaB_6.[1]

Since the 1960s, LaB_6 cathodes have been extensively studied and optimized. Other similar compounds were studied until 1979, when Storms and Mueller determined that LaB_6 was the most effective low work function Lanthanum Boride compound.[29] Gallagher found that LaB_6 is more resistant to poisoning at higher temperatures,[30] Futamoto, et al. studied a single crystal LaB_6 cathode that showed that evaporation rate and emission current are dependent on temperature and pressure,[31] and Goebel and Chu found that increasing the size of the insert can increase the output current.[8] Van Noord, et al.[32] analyzed the effects of thickening the hollow cathode walls in the emitter region. The goal was to increase thermal conduction and decrease variations in temperature. The reduction in temperature variations improved the uniformity of emission and plasma density.

Additionally, this study showed that increasing the emission area by increasing the insert diameter could increase the lifetime to 100 kh at 50 A of discharge current.

2.6 Hollow Cathode Variations

A variety of other cathode variations have been designed without heaters and/or inserts. Mirtich developed a mercury based hollow cathode that used 100 W to produce 15 A, and had 4 kh of life.[33] While this provided high current, the lifetime is not long enough for most EP applications, which require hundreds of thousands of hours.[16] Aston developed a heaterless, insertless cathode using an ignitor plug and an annular semiconductor to break down the propellant and create a plasma plume, as shown in Figure 2.3.[34]

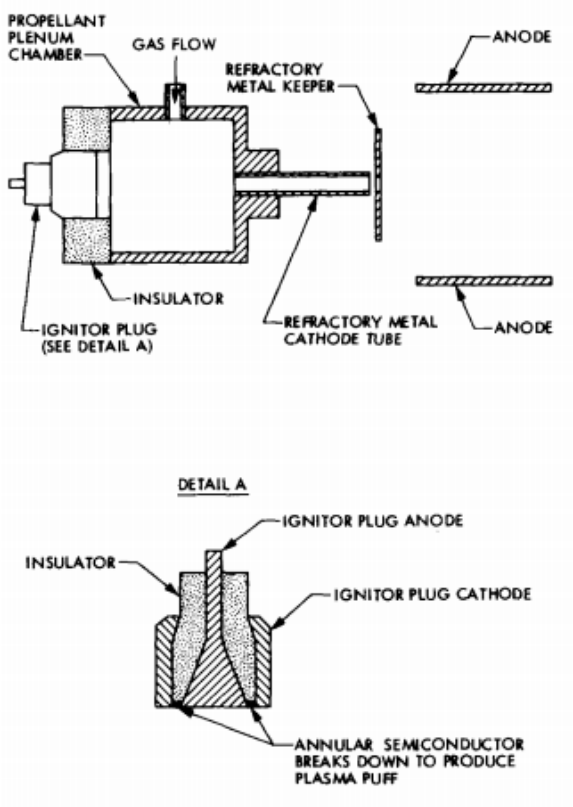

Figure 2.3. Aston's heaterless, insertless cathode.[34]

This device only required 10-20 Watts of startup power, but was highly unstable and could not sustain a discharge for more than a few seconds.

Schatz studied a heaterless cathode that required a high amount of propellant.[35] This device worked by flooding a chamber between two electrodes, then increasing the voltage until breakdown of the propellant was achieved. Once the cathode ignites, the flow rate is reduced to sustain the discharge. This can be seen in Figure 2.4.

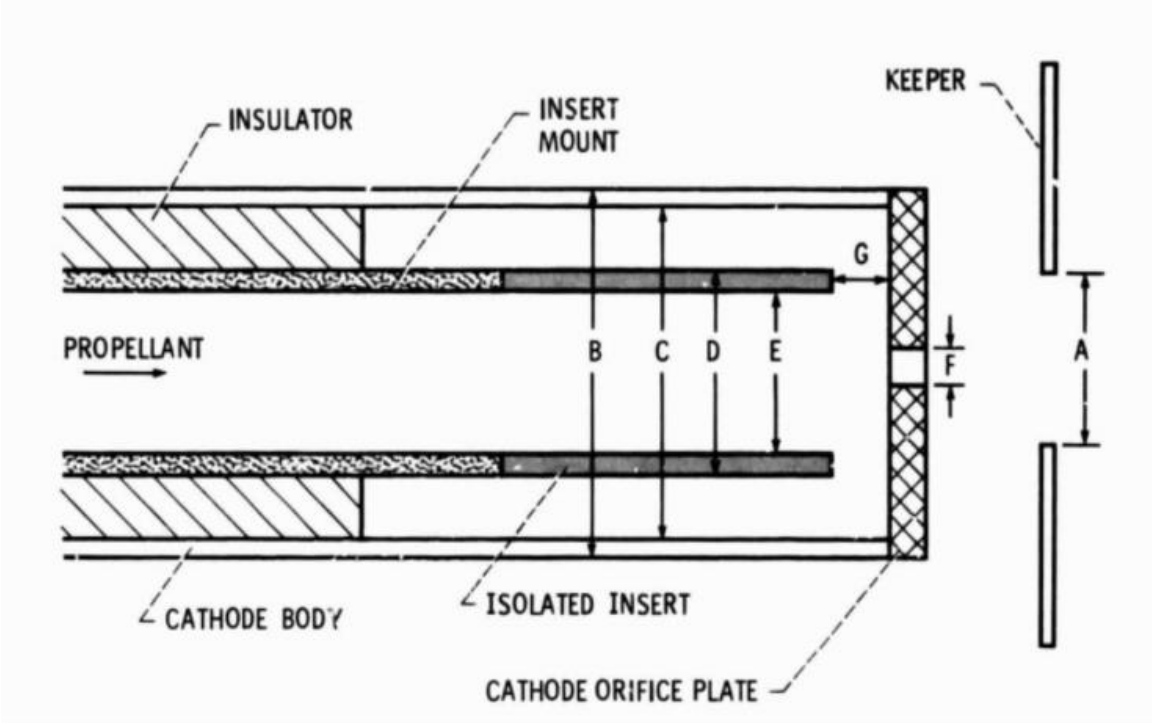

Figure 2.4. Schatz' heaterless cathode design[35]

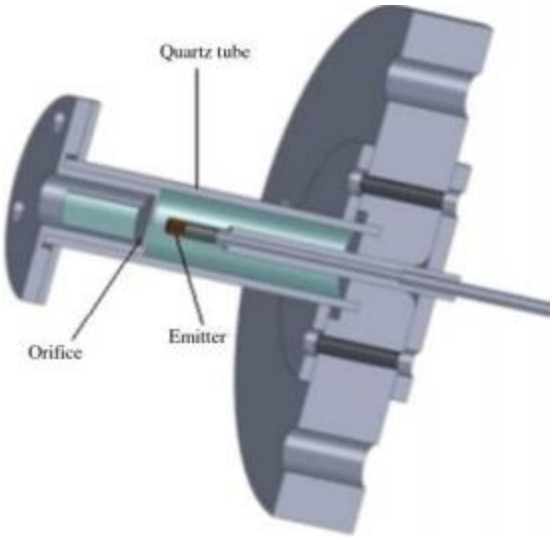

Figure 2.5. Heaterless cathode with emitter orifice breakdowns.[36]

Vekselman, et al. also developed a heaterless cathode using emitter-orifice-plate-gap breakdowns, as shown in Figure 2.5.[36] This cathode can achieve millisecond ignition with less than 30 W of power. Using xenon, 0.5 to 1.5 A of discharge current can be extracted. These cathodes experienced a high amount of erosion, which limits their lifetime.

Rand and Williams developed a variation called the electride cathode. An electride structure uses positively charged "cages" to trap electrons across the material, as shown in Figure 2.6.[37,38] Once the density of the electrons is high enough, the material becomes conductive. When a high temperature is applied, the electrons are released, making the material useful as a cathode insert.

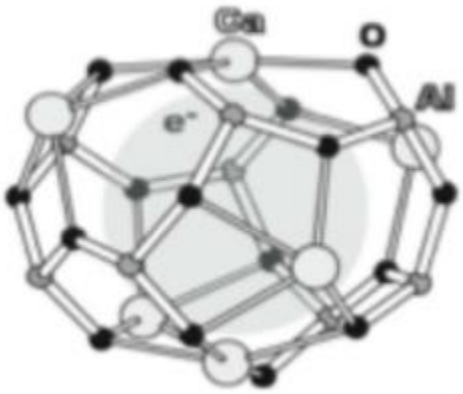

Figure 2.6. Electride Hollow Cathode Lattice Framework.[38]

This device is a heaterless cathode that uses the calcium-aluminate phase 12CaO-$7Al_2O_3$ (C12A7) as an insert material. This material has a low work function of 0.6 eV, which makes it well suited for electron emission in electride form. The electride cathode works by pumping high amounts of xenon or iodine (30-50 sccm) over the C12A7 insert and ionizing it with a 1 kV supply. Once the cathode ignites, the keeper switches to a current-limited mode and holds the output at 0.3 A. The flow rate is then decreased to around 10 sccm. This cathode can produce a discharge current between 3 and 15 A.

In 2017, Caruso and McDonald found that the performance of these C12A7 inserts is dependent on the manufacturing method.[39] It was found that during the annealing process, exposing the insert to higher temperatures would allow for higher current densities in operation. Additionally, longer annealing times led to lower performance of the insert. Drobny, Tajmar, and Wirz also found that C12A7 cathodes will overheat rapidly if operated at higher currents.[40] It was found that when operated at an emission current lower than 2 A, this type of cathode can only be used for 5 minutes at a time before overheating.

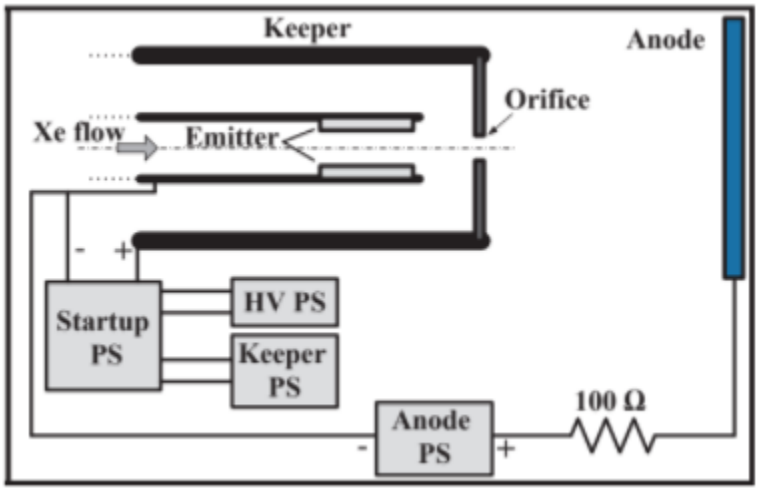

Figure 2.7. Heaterless Hollow Cathode Design.[41]

Most recently, Lev, et al.[41] developed a heaterless cathode that uses high voltage pulses to ignite a plume inside the keeper. The plume itself then heats the insert to emission temperature, at which point the plume is drawn out by the anode, as shown in Figure 2.7.

This cathode produces up to 1 A of emission current while using less than 40 W of power. However, the lifetime and performance of the cathode is still limited by the degradation of the insert material. After only a few hours of operation at current above 0.7 A, the cathode orifice became clogged and the insert rapidly deteriorated.

2.7 Radio Frequency Cathodes

Electric propulsion devices need long lifetimes to provide a clear advantage over traditional chemical propulsion methods. However, some components of EP devices, including hollow cathodes, are limited to 25-30 khrs. This lifetime limitation is due to the deterioration of the elements of the cathode, mainly the insert and the heating elements. To obtain high discharge currents, hollow cathodes have high ion production. However, high ion production leads to ion bombardment. Ion bombardment is a significant contributor to

cathode erosion, and therefore a major factor in determining cathode lifetime.[42] The inserts in hollow cathodes also require a preheating phase to properly operate, which prevents quick ignition of the cathode and delays the use of the propulsion devices.[6] RF cathodes provide an alternative that can both provide instant ignition and extend the lifetime of the propulsion devices.[17]

Most RF cathodes are built similarly to DC hollow cathodes. However, they replace the heater with an RF coil and the insert with an ion collector, as shown in Figure 2.8 and Figure 2.9. They operate by pushing a neutral gas through the discharge chamber, where the RF-induced field ionizes the gas and pulls the ions to the negatively biased ion collector while an anode pulls the electrons through the orifice.

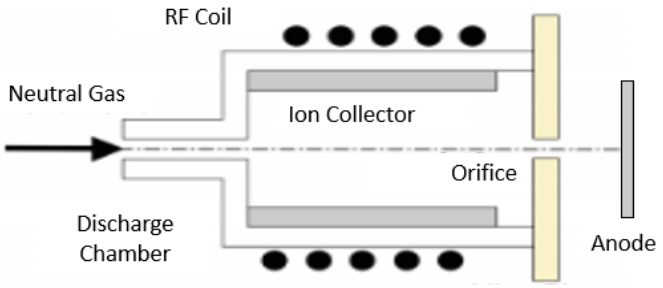

Figure 2.8. Schematic of an RF Cathode.

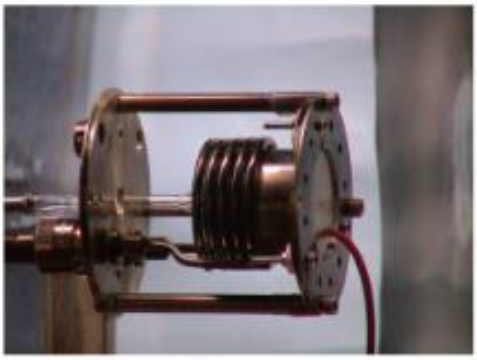

Figure 2.9. Hatakeyama's RF Cathode.[6]

RF cathodes produce comparable current densities to hollow cathodes. Numerous RF sources can be used, varying from magnetic field dependent electron cyclotron resonance (ECR) and helicon sources to the magnetic field independent capacitive and inductive sources. Helicon sources are the most effective for RF cathodes due to the ability to produce high plasma densities (10^{13} cm^{-3}). The drawback of this source is that it also requires high external magnetic field strengths and RF powers. Inductively coupled plasmas can produce plasma densities of 10^{10} to 10^{12} cm^{-3}, which is sufficient for most needs. Inductively coupled sources also require a much smaller magnetic field, making them more favorable than the helicon sources.[17]

Many RF cathodes have been developed with varying current and power ranges. Longmier tested an RF cathode that produced 3.75 A of extraction current using 340 W of power.[17] Williams, et al. created a similar device that could draw current from 3 to 17 A at powers of 400 to 1600 W.[18] Hatakeyama studied a smaller cathode that could produce 1.7 A of extraction current for only 80 W.[6] Similarly, Jahanbakhsh and Celik used an inductively coupled design that produced 1.2 A and required 100 W of power.[43,44] Weis, et al. developed a capacitively coupled design that produced a much smaller 0.1 A for around 100 W.[45] This design required creative developments. Weis's device had a low plasma density, which required a large orifice to achieve high extraction currents. However, the orifice size was limited by the desire for a low consumption of gas. A plasma "bridge" had to be created to carry the electrons out of the orifice to the anode.

A low frequency inductively coupled RF cathode was created by Raitses, et al.[46] The idea is similar to an arcjet, but in the RF-cathode, the circuit is closed only by the ion current to the cathode chamber walls. The electrons are extracted through an opening in

the chamber walls. If the electron current through this opening exceeds that of the ion saturation current at the wall, the ion Bohm current limits that maximum electron extraction current.

Similar cathodes have been tested including helicon-based RF cathode,[47] ECR discharge cathode,[48] and an inductively coupled plasma (ICP) cathode.[49] In the ICP cathode developed by Godyak, a highly efficient electron extraction cost was achieved, with a current-to-power ratio of 40 W/A. In Raitses's cathode, similar efficiencies were found. However, if the extraction voltage is included, this cost increases to 85 W/A.[46]

2.8 Waveguide Cathodes

Getty and Geddes first used permanent magnets and waveguide coupling to create electron cyclotron resonance plasma in 1998.[50] By placing the magnets such that the magnetic field is perpendicular to the microwave propagation, the plasma's extraordinary wave reaches upper hybrid frequencies. This maximizes efficiency in power absorption, but usually comes at a loss in plasma density. However, by heavily isolating the plasma and increasing the bulk ionization, an over dense plasma is created. This cathode used 200-700 W of power, but was not used as an actual neutralizing device.

The use of a magnet waveguide to create plasma in a cathode was studied by Hidaka, et al.[51] Permanent magnets were used to create an electron cyclotron resonance plasma. This cathode has no physical "antenna" that is present in hollow cathodes. It is a heaterless, insertless device, but requires a microwave source and strong magnets. Using 200 W of microwave power, 1 A of extraction current was produced. Weatherford, et al.[52] developed

a similar, more efficient device. It was able to achieve extraction currents over 4 A with a power input of only 120 W.

An alternative cathode was studied by Plasek, et al.[53–55] It was found that a bulk emitting cathode can be enhanced by an RF waveguide. This cathode uses RF technology to maximize the emitter area in a thermally-limited region of a LaB_6 cathode. This minimizes the space-charge limited emission and therefore allows the emitter to be fully utilized. For a given flow rate, the RF power and waveguide length can be adjusted to cause a sharp increase in the electric field magnitude and plasma density. The addition of the RF waveguide can greatly increase the maximum discharge current. This cathode can produce 160 to 200 A of current for only 100-300 W of power. However, the flow rate ranges from 40-215 sccm, which is higher than desired for most cathodes.

Chapter 3

EXPERIMENTAL METHODS

Research is what I'm doing when I don't know what I'm doing.
– Wernher von Braun

3.1 Experimental Setup

Two experimental setups were used to study the operation of the microplasma heaterless cathode (MPHC). Electrical schematics for these two experiments can be seen in Figure 3.1 and Figure 3.2. The main differences between the two setups are the use of an anode or Langmuir probe, and the use of an external collar or the ion collector as the negative electrode. A picture of the MPHC can be seen in Figure 3.3. Both experiments used ac and pulsed dc supplies. A commercial plasma ball was used as the ac supply and output a constant ac signal of 12 kV with a 1 μs pulse width and 11 kHz frequency. The pulsed dc supply was controlled by a high voltage pulse generator and digital delay generator and allowed for variation in voltage, pulse width, and frequency.

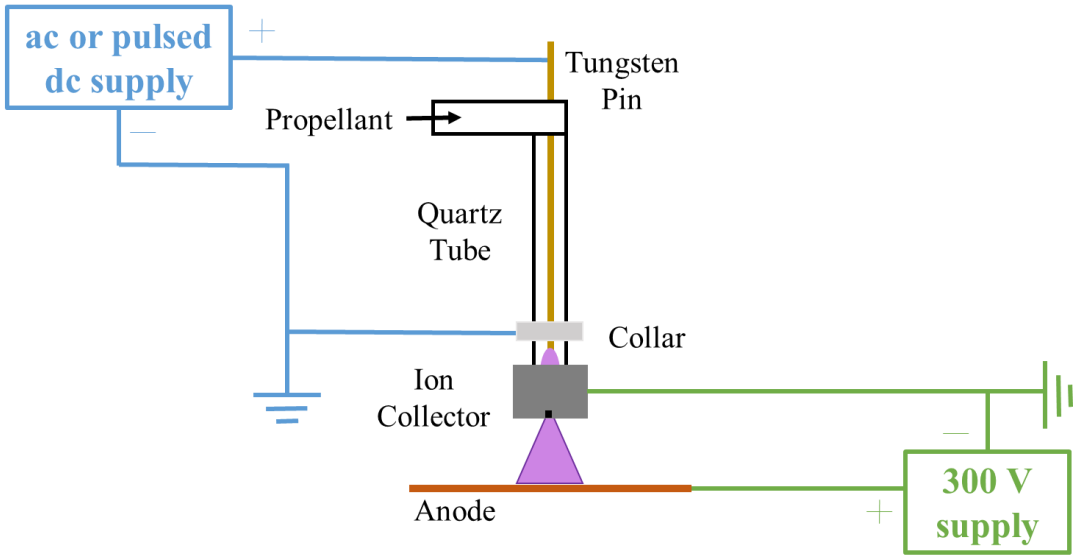

Figure 3.1. Electrical schematic of cathode. The design consists of two independent circuits.

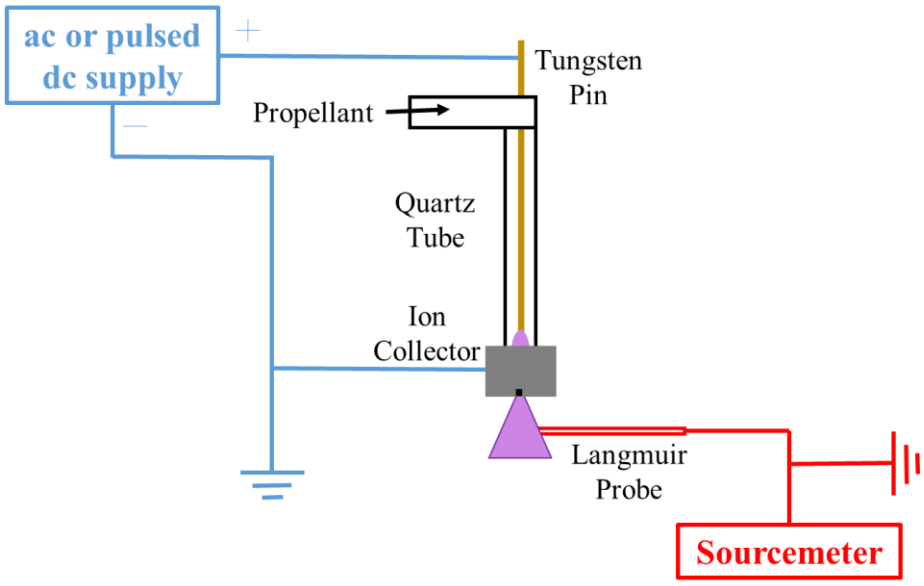

Figure 3.2. Electrical schematic of Langmuir probe tests.

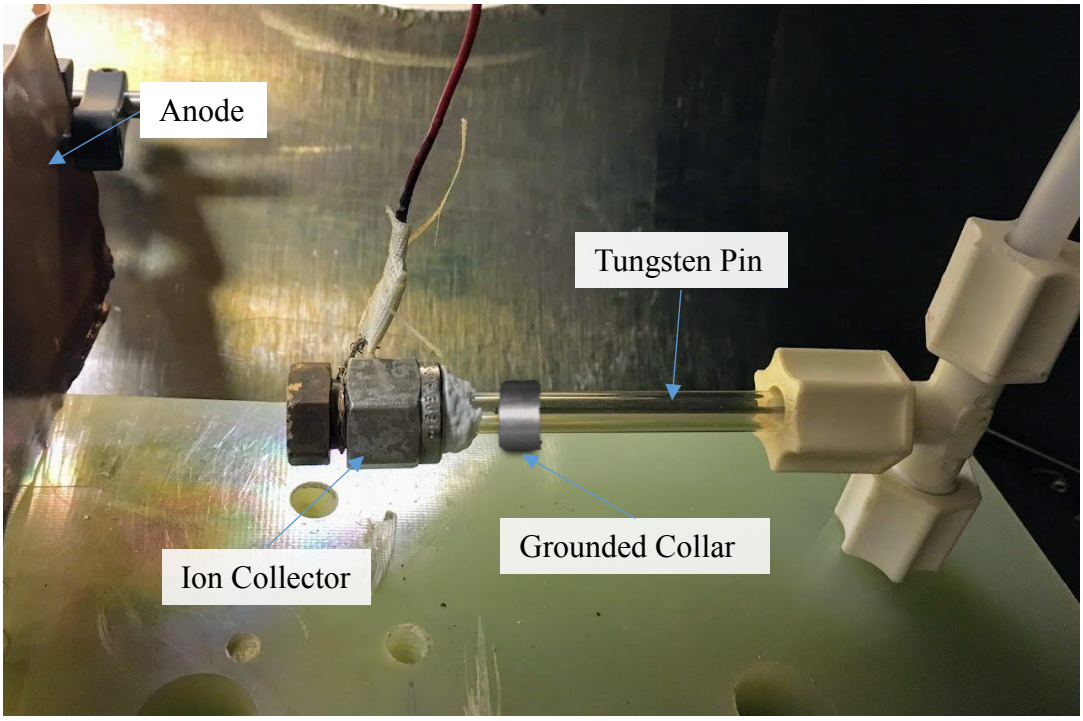

Figure 3.3. The MPHC setup showing the collar, anode, ion collector, and tungsten pin. The clear tube which the collar sits around is the 6 mm OD quartz tube in this picture.

The cathode was developed by inserting a 1 mm tungsten filament into a quartz tube. For initial tests, the quartz tube diameter was varied in the tests with either a 6 mm OD or ½" OD tube and different IDs. A steel collar was placed around the outside of the quartz tube and the microplasma was generated with an ac or pulsed dc power source connected to the central filament and external collar. A brass ion collector was placed on the end of the tube and connected to the negative terminal of a separate 300 V dc supply, while a plate anode was placed a short distance away and biased positively. Argon was used as the working gas and ionized by the induced field, then separated by the ion collector and anode. The flow of electrons into the anode produced a variety of currents.

Additional testing was done with Langmuir probes placed in the cathode plume to obtain measurements of the plasma properties. For these tests, the probe replaced the anode, the

300 V dc supply was not used, and the collar was removed. The probe was controlled with a Keithley 2400 sourcemeter.

3.2 Equipment

All tests were conducted in the small vacuum chamber at the Plasma and Electrodynamics Research Lab (PERL) at UAH. The chamber is 1 ft in diameter and 2 ft long and is pumped with a mechanical pump and a magnetically levitated turbopump. The turbopump was used to achieve high vacuum conditions that simulate the operating space environment. The chamber has a base pressure of 2×10^{-6} Torr, with operating pressures reaching 4×10^{-4} Torr-Ar for higher flow rates. The chamber can be seen in Figure 3.4.

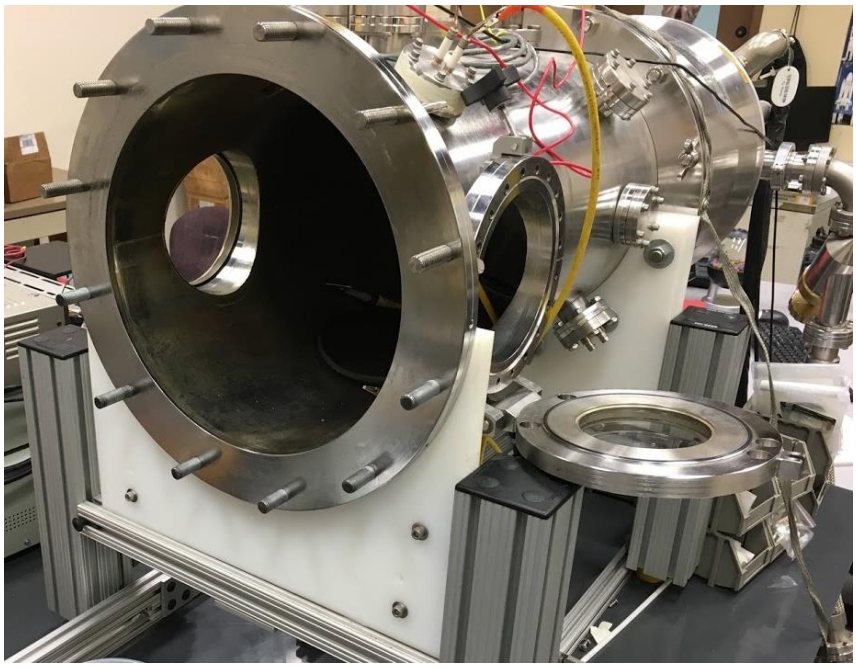

Figure 3.4. Vacuum Chamber.

The argon flow rate was controlled using a 100 sccm MKS mass flow controller. Vacuum pressures were read using an Instrutech Hornet ion gauge pressure sensor. The sensor is calibrated for air, so the pressure readings were adjusted for argon using Equation 3.1.

$$P_{Ar} = \frac{P_{air}}{1.29} \tag{3.1}$$

The pulsed dc voltage was provided by a Matsuada 10 kV supply and controlled by a DEI PVX-4110 Pulse Generator and a Stanford Research Systems DG645 Digital Delay Generator. The ac signal was provided directly by a modified commercial plasma ball. The anode was controlled by a GW Instek 300 V variable dc supply.

Double Langmuir probes were used to measure the electron temperature and density in the plume. Single probes could not take useable measurements due to "linking" between the probe and the plume and the operating conditions of the cathode. This phenomena gave false readings, preventing the use of single probes. The double Langmuir probes used in this experiment were created using 0.127 mm (0.005 inch) tungsten filaments. The filaments were placed in isolated channels of a 2.4 mm diameter alumina tube with 1.3 mm of separation between the filaments. They then extended to 2 mm outside one end of the tube and were each pressure fit with an external wire on the opposite end. The external wire was then taped in place with Kapton electrical tape and connected to the sourcemeter. This can be seen in Figure 3.5.

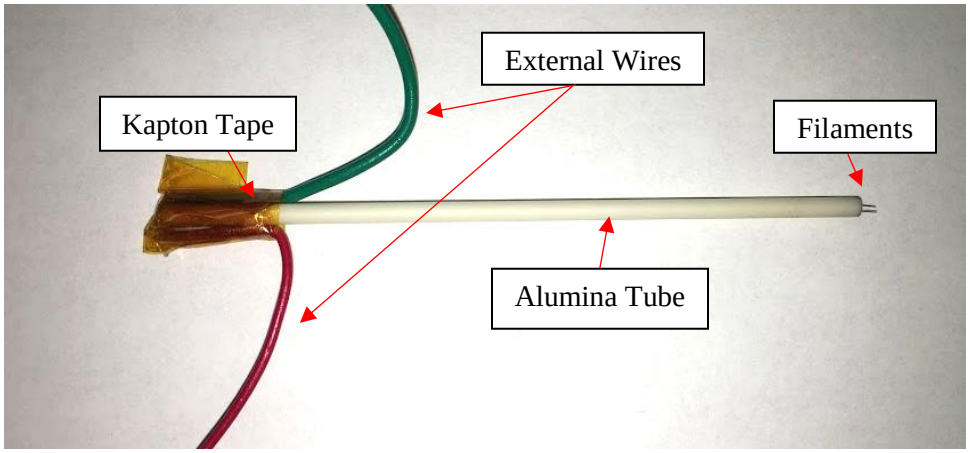

Figure 3.5. Example double probe used in this experiment.

3.3 Langmuir Probe Theory

Plasma characteristics such as electron temperature and density can aid in predicting the capabilities of the cathode. Langmuir probes are well suited for this type of measurement. Additionally, knowing plasma density can aid in predicting the degradation of cathode elements. Higher density regions are likely to degrade more rapidly than other regions. Measurements can be made with either single probes or double probes to determine these characteristics. Single probes are best for determining ion density, while double probes are best suited for finding electron temperature and electron density.[56]

Probe analysis assumes a collisionless plasma, meaning that the Debye length is less than the ion-neutral mean-free-path. This assumption holds true at low pressures, as shown in Equation 3.2, which allowed for the use of Langmuir probes in this experiment.

$$\lambda_D = \sqrt{\frac{\epsilon_0 k_B T_e}{n_e q^2}} < \frac{1}{P} \sim MFP \tag{3.2}$$

For an assumed electron temperature of 4 eV and an electron density of 10^{16} m^{-1}, the Debye length is approximately 10^{-4} m. For a pressure of 5 x 10^{-5} Torr (.0067 Pa), the ion-neutral

mean-free-path is on the order of 150 m. This is much larger than the Debye length, allowing for the assumption of collisionless plasma.

In each test, a double probe was placed 5 mm from the cathode orifice and biased from -100 to 100 V using the sourcemeter. The filament current was measured and used to calculate electron temperature and density. Equation 3.3 shows that the change in current at 0 volts can be found using electron temperature, T_e, and the ion and electron saturation currents, i_1, and i_2, respectively,[56]

$$\left.\frac{dI}{dV}\right]_0 = \frac{e}{kT_e}\frac{|i_1|*i_2}{|i_1|+i_2} \tag{3.3}$$

where e is electron charge and k is Boltzmann's constant. This equation can be rearranged to solve for T_e, as shown in Equation 3.4.

$$\frac{1}{T_e} = \left.\frac{dI}{dV}\right]_0 \frac{k}{q}\frac{|i_1|+i_2}{|i_1|*i_2} \tag{3.4}$$

The change in current at 0 volts and saturation currents can be found by using an I-V plot, as shown in Figure 3.6.

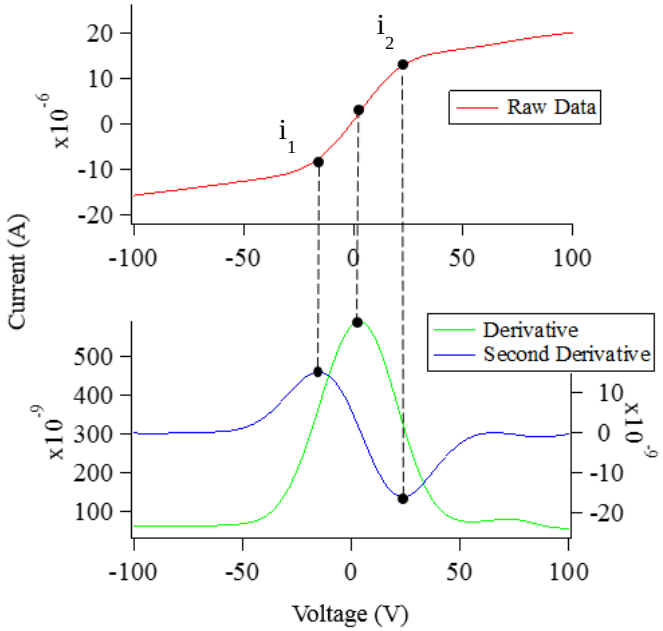

Figure 3.6. Sample graph for calculating T_e.

The desired values can be found by calculating the first and second derivative of the data. A smoothing function must be used to give accurate first and second derivatives. This function takes the averages of surrounding points to generate a smooth curve for the original data set. The peak of the first derivative is the inflection point of the original curve. The slope is calculated from +/- 5 volts from this inflection point to find the change in current at 0 volts. The peaks of the second derivative correspond to the negative and positive saturation currents, i_1 and i_2, respectively.

Under the assumption of quasi-neutrality, the ion density should be approximately equal to the electron density. Therefore, calculating the ion density will also give the electron density. Equation 3.5 shows the current relation to ion density, n_i,

$$I = \frac{1}{2} q n_i A_p \left(\frac{kT_e}{2\pi M}\right)^{\frac{1}{2}} \tag{3.5}$$

where A is probe area and M is the mass of argon atoms. Rearranging to find n_i gives Equation 3.6.

$$n_i = \frac{2I}{qA_p\left(\frac{kT_e}{2\pi M}\right)^{\frac{1}{2}}} \tag{3.6}$$

The results of these calculations were used to characterize and compare operating conditions of the cathode.

For all measurements, error was taken into account. Electromagnetic interference, arcing, and fluctuations in pressure could all cause errors in probe measurements. To reduce the EMI and arcing errors, cables were shielded with aluminum foil and open connections were shielded with rubber fusion tape. To reduce pressure variation, the flow rates remained consistent and the pressure was closely monitored using the ionization gauge.

Furthermore, the cathode temperature varied in each test due to length of operation. Efforts were made to decrease this variation by shortening the length of each test. However, this did not eliminate the problem. This variation was taken into account by adding error bars to all calculations.

3.4 Theoretical Models

A theoretical model can be used to calculate the plasma density and thus current from the microplasma cathode for comparison to probe and current measurements. The model is based on the power model described by Lieberman and Lichtenberg[57] for a cylindrical plasma as shown in Figure 3.7 for the MPHC. The region of interest is between the pin and orifice where the microplasma is formed with a radius *R* and length *l*.

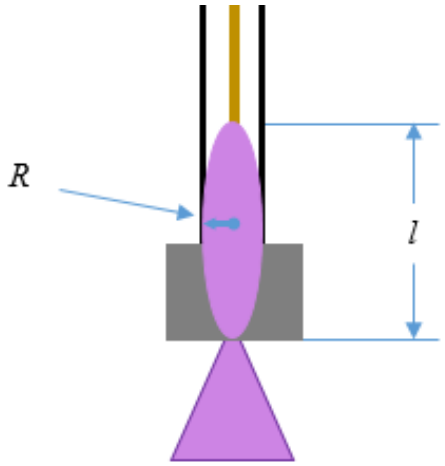

Figure 3.7. Visualization of the power model.

The power output of a system can be given as a function of plasma density (n_0), electron charge (e), Bohm velocity (u_b), plasma area (A_{eff}), and energy loss (ε_T). Assuming the input power is equal to the power absorbed by the plasmas (P_{abs}), the power balance can be

written as shown in Equation 3.7. If the input power is known, the theoretical plasma density can then be found from Equation 3.8.

$$P_{abs} = n_0 \mathrm{e} u_b A_{eff} \varepsilon_{\mathrm{T}} \tag{3.7}$$

$$n_0 = \frac{P_{abs}}{\mathrm{e} u_b A_{eff} \varepsilon_{\mathrm{T}}} \tag{3.8}$$

The absorbed power can be approximated as the input power which is calculated from the input voltage and current. The Bohm velocity, which is the minimum velocity at which ions can enter a plasma sheath, can be found using Boltzmann's constant (k), electron temperature (T_e), and ion mass (M).

$$u_b = \sqrt{\frac{kT_e}{M}} \tag{3.9}$$

The energy loss, which is the difference between the absorbed power and the output power, can be calculated as a function of collisional (ε_c), ion ($2T_e$), and electron energy losses ($5.2T_e$). Collisional energy is lost when electrons and ions collide and create a pair. Ion and electron energy losses are a direct result of the contact of ions and electrons with the walls. The calculation of total energy loss is shown in Equation 3.10.

$$\varepsilon_T = \varepsilon_c + 2T_e + 5.2T_e \tag{3.10}$$

In this case, the plasma is assumed to be collisionless, causing the ε_c term to be negligible. The plasma area can also be found using Equations 3.11-14,

$$A_{eff} = 2\pi R^2 h_l + 2\pi R l h_r \tag{3.11}$$

$$h_l = \frac{0.86}{\left(3+\frac{l}{2\lambda_i}\right)^{\frac{1}{2}}} \tag{3.12}$$

$$h_R = \frac{0.8}{\left(4+\frac{R}{\lambda_i}\right)^{\frac{1}{2}}} \tag{3.13}$$

$$\lambda_i = \frac{1}{330P} \tag{3.14}$$

where l and R are the plasma length and radius, respectively, h_l and h_R are edge-to-center ratios, λ_i is the ion-neutral mean-free-path, and P is the operating pressure in Torr. By assuming that the total electron flux is constant, and knowing the exit area of the quartz tube (A_T), an estimation can be made of the maximum current produced in the quartz tube.[16] This is shown in Equation 3.15.

$$\mathrm{I} = A_T q n_e \left(\frac{8kT_e}{\pi M}\right)^{\frac{1}{2}} \tag{3.15}$$

Chapter 4

RESULTS

Research is formalized curiosity. It is poking and prying with a purpose.
– Zora Neale Hurston

Tests were conducted to study the operation of the MPHC. The first method of characterizing performance was measuring current output, thus extracted electron current, from the anode power supply. This readout was recorded for each experiment with different tube sizes and flow rates. Langmuir probes were used to measure electron temperature and density in a plasma.

4.1 Cathode Sizing

The effect of the quartz tube ID, thus the cross-sectional area, was tested first. Tests were done with 2, 3, 4, and 6 mm ID quartz tubes all 80 mm in length. The tests were run with the ac source and 300 V on the anode at different argon flow rates. The results are shown in Figure 4.1 which shows the extracted electron current on the anode as a function of flow rate and tube ID. It was found that the current increased with both flow rate and tube ID.

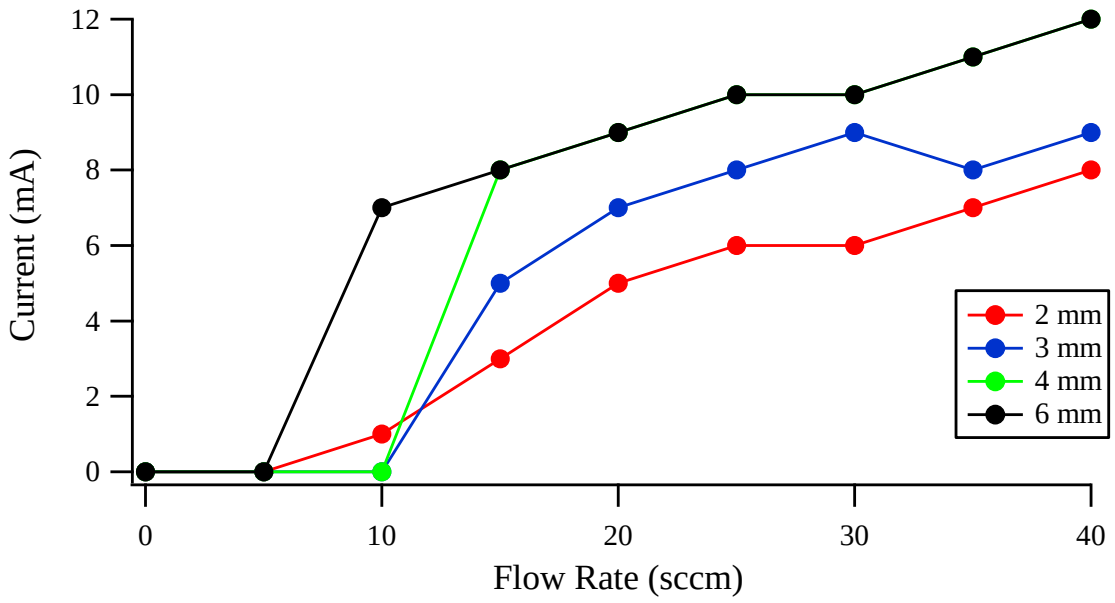

Figure 4.1. Comparison of operation. The lines denote different quartz tube inner diameters.

Further tests were conducted with 8 and 10 mm ID tubes and showed that performance stalled out at 6 mm. The plume ignited in the 8 and 10 mm tubes, but no current was extracted. This is most likely related to a decrease in the density of the gas for larger IDs given the same flow rate. The larger ID tubes have larger free volumes, allowing the plume to expand in the tube instead of at the anode. Additionally, the pressure within the tube is theoretically lower in the higher ID tubes. Goebel and Katz found the pressure relation with tube size for a cathode, as shown in Equation 4.1,[16]

$$P = \left(\frac{0.78 Q \zeta T_r l}{d^4}\right)^{\frac{1}{2}} \tag{4.1}$$

where P is the pressure in Torr, Q is the flow rate in sccm, ζ is the viscosity of the propellant gas in poise, T_r is the temperature ratio given as T_g/289.7 K, l is the tube length, and d is the tube diameter. Holding all else constant, it can be seen that changing the diameter of

the tube causes a quadratic change in the pressure. In this case, the 2 mm tube had pressures of 7 Torr (933 Pa), while the 8 mm tube had pressures of 0.5 Torr (67 Pa). For the higher ID tubes, this pressure differential prevented the plume from physically reaching the anode at the same conditions as the lower ID configurations.

While there was minimal difference in performance between the 4 mm and 6 mm tubes, the 4 mm tubes proved to be more adaptable. The tubes with a 6 mm ID had a ½" OD, while the 4 mm tubes had a 6 mm OD. The larger OD led to difficulties with the cathode designs. More configurations could be used with the 4 mm tubes. From these results, all future tests used the 4 mm tube configuration.

4.2 Probe Measurements

Several Langmuir probe measurements were taken to determine the properties of the ac source plasma. Three flow rates were tested, 25, 30, and 35 sccm. Figure 4.2 shows the raw double probe current-voltage curves obtained. It can be seen that at positive voltages, the saturation current increases with flow rate. This is due to the higher density of particles available for ionization. Using Equations 3.4 and 3.6, the electron temperature and density for the ac source were found, as shown in Figure 4.3.

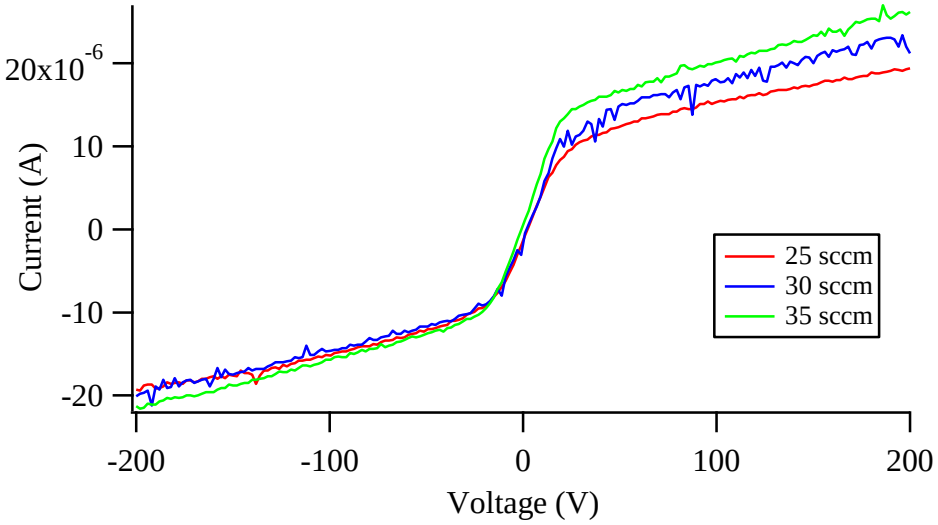

Figure 4.2. I-V curve for ac generated plasma at various flow rates.

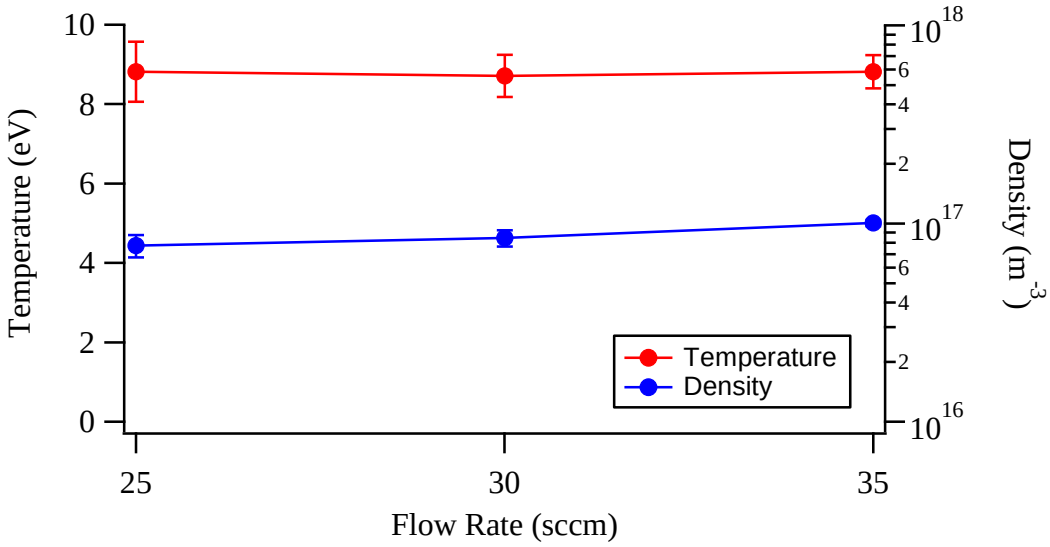

Figure 4.3. Ac generated plasma properties.

While the changes in flow rate did not affect electron temperature, an increased flow rate led to a minor increase in electron densities. Because the gas is the source of electrons, more flow allows for more ionization and therefore denser electrons.

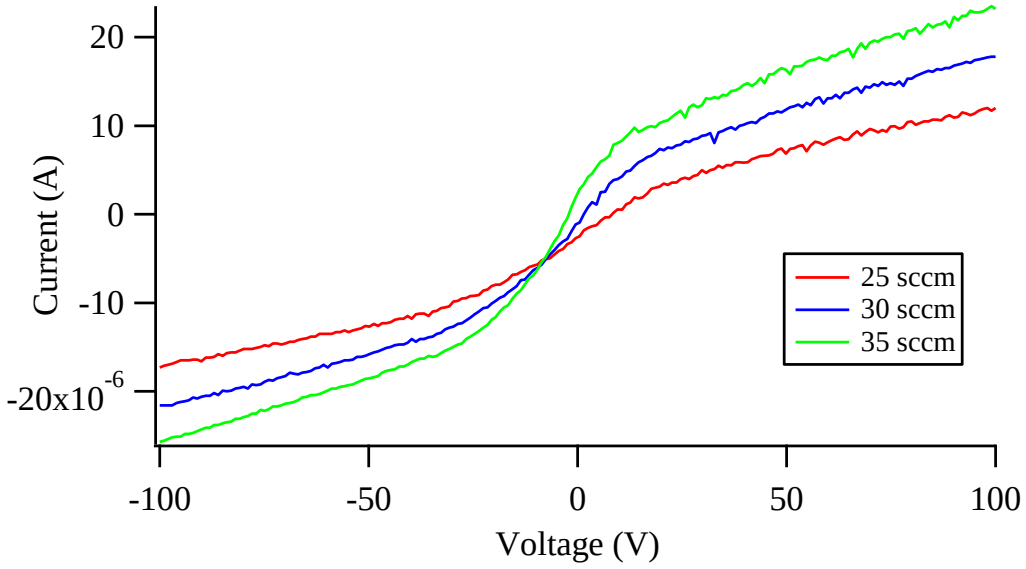

Figure 4.4. I-V curve for pulsed dc generated plasma at various flow rates.

The ac source cannot be varied, so flow rate is the only variable. The pulsed dc source provides more opportunities for optimization. Tests with the pulsed dc system allowed for variation in pulse width, frequency, and voltage in addition to variation in flow rate. After varying each of these, it was found that the most stable testing condition was a pulse width of 400 ns, frequency of 7 kHz, and voltage of 1.4 kV. The results from these tests can be seen in Figure 4.4.

As with the ac supply, the magnitude of the current steadily increases with flow rate. Equations 3.4 and 3.6 were used again to calculate the electron temperature and density for the unshielded cathode with an ion collector. The trends in electron temperature and density are shown in Figure 4.5.

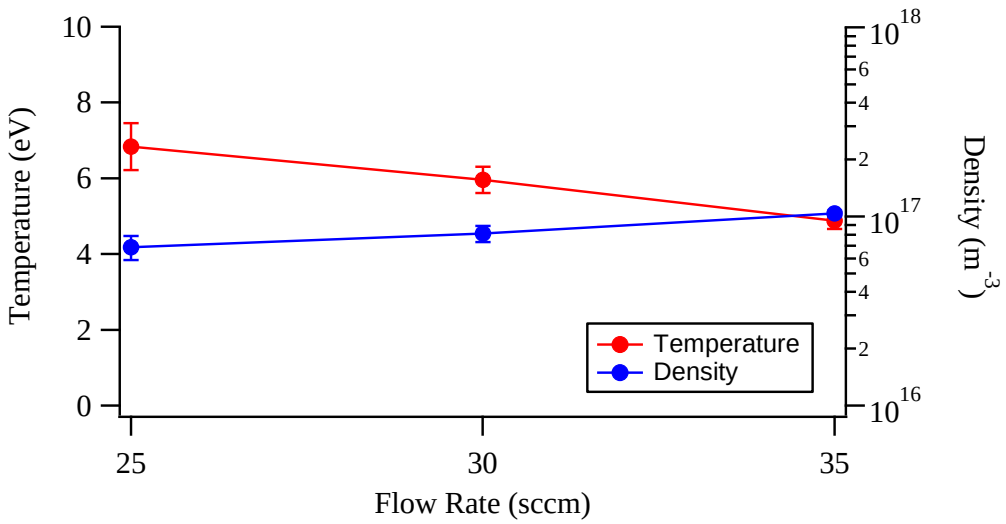

Figure 4.5. Pulsed dc generated plasma properties.

While these conditions produced the steadiest plume, other conditions were also studied. The effects of varying voltage, pulse width, and frequency were explored. To study each of these, the flow rate was held constant at 30 sccm and each was varied individually. First, the voltage was set to 1.1 kV and 1.4 kV while the pulse width and frequency remained at 400 ns and 7 kHz, respectively. This resulted in the changes shown in Figure 4.6.

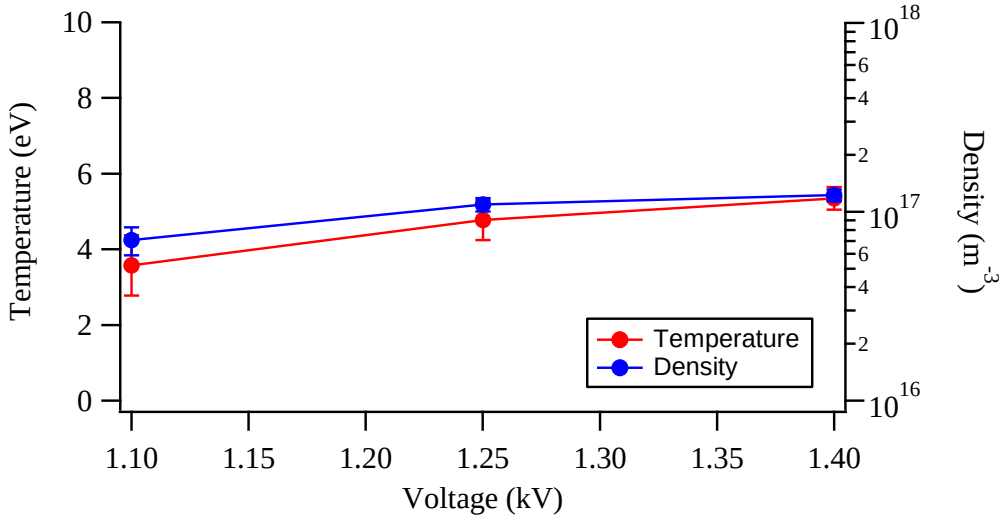

Figure 4.6. Variations in the input voltage to the cathode.

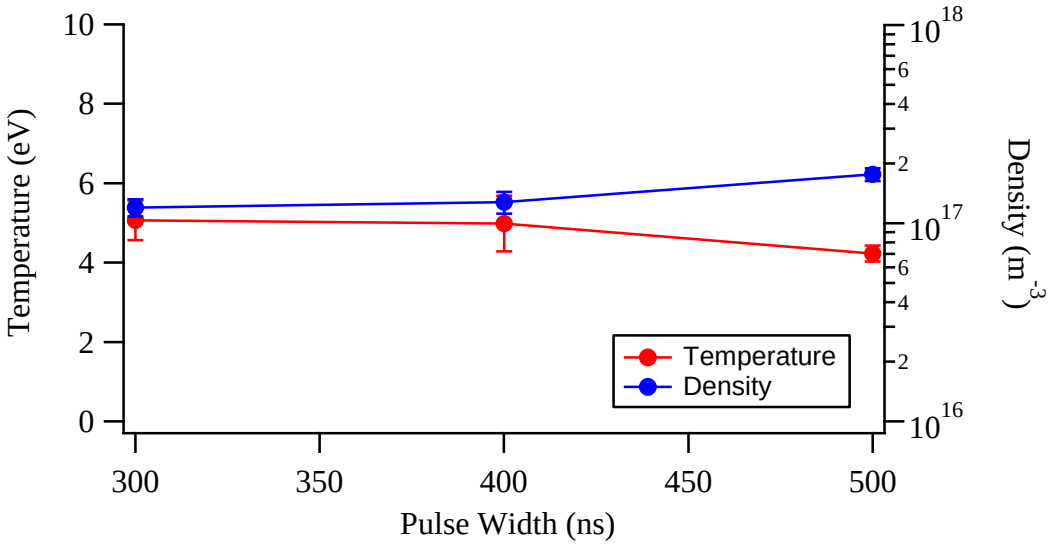

Figure 4.7. Variations in pulse width.

Increasing the voltage to the cathode increased the electron temperature and density. With more power in the system, more ionization occurs. Increased ionization usually results in higher densities and lower temperatures, but increased power leads to higher temperatures as well. For the next test, the pulse width was set to 300 and 500 ns while the voltage remained at 1.25 kV and the frequency at 7 kHz. This resulted in the plot shown in Figure 4.7.

Varying the pulse width caused opposing changes in temperature and density. Higher pulse widths led to higher densities, but lower temperatures. Longer pulses led to more ionization due to the increase exposure time. With the energy in the system remaining constant, temperatures decreased to compensate for this increase in density.

Finally, the pulse width was held at 400 ns and the voltage at 1.25 kV while the frequency was varied to 6 kHz and 8 kHz. These results are shown in Figure 4.8.

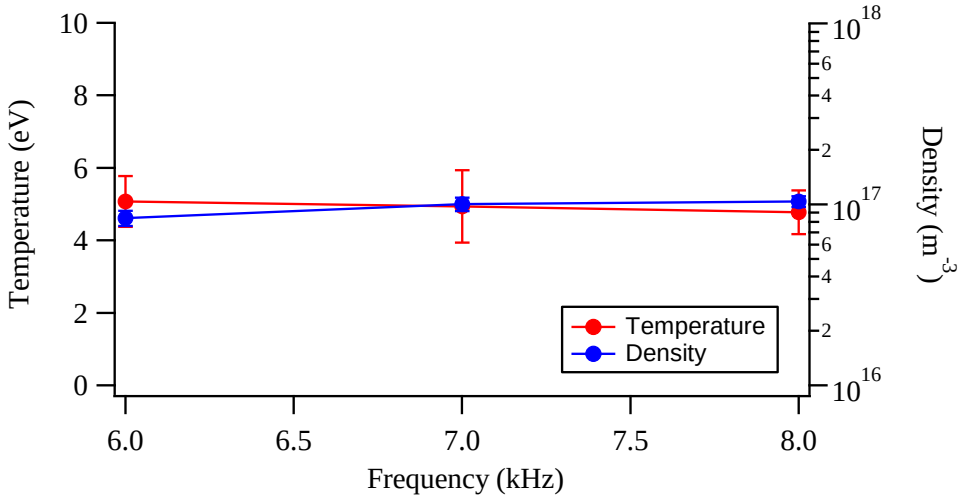

Figure 4.8. Variations in frequency.

Frequency had less of an effect on temperature than the other factors, but followed the same trends with density. As frequency increased, temperature decreased from 5.1 to 4.8 eV. However, the uncertainty in this set of temperature measurements (+/- 1 eV) was greater than the change of 0.3 eV. On the other hand, density increased from 8.4×10^{16} to 1.0×10^{17} m^{-3} which exceeded the uncertainty of +/- 8×10^{15} m^{-3}. As the pulses become more frequent, more ionization occurs in a shorter time, leading to higher densities.

4.3 Observed Limitations

For each increase in voltage, pulse width, frequency, or flow rate, the plume also becomes visually brighter, as shown in Figure 4.9. However, this increase was limited by the stability of the discharge. As the plume became visibly brighter, it would frequently transition into arc mode, where high power electric streams would link to surrounding equipment. This was very damaging for the equipment, so operation in this mode was limited.

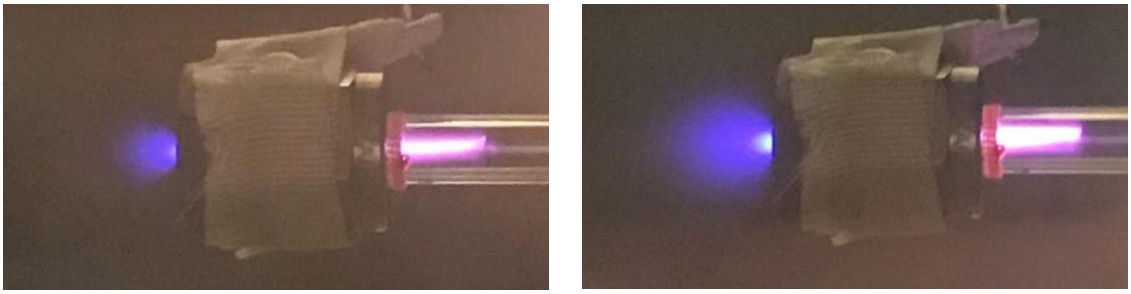

Figure 4.9. Changes from a weaker (left) to a stronger (right) plume.

Furthermore, it was found that each variable could be further increased as the others decreased. For example, at a flow rate of 30 sccm, a pulse width of 200 ns, and a frequency of 5 kHz, voltages of 6 kV could be achieved with a stable plume. Table 4.1 shows the most stable regions at the maximum studied value of each condition.

Table 4.1. Stable operating condition at the maximum studied value for each variable.

Flow rate (sccm)	Voltage (kV)	Frequency (kHz)	Pulse Width (ns)
35	1.5	7	400
30	6	5	200
30	1.25	10	300
30	1	5	1000

4.4 Hall Thruster Testing

Early testing of the MPHC with a miniature Hall Thruster produced limited success. The setup and operation of this experiment can be seen in Figure 4.10. While a strong plume was drawn from the cathode into the thruster channel, currents above 10 mA could not be sustained. It is believed that currents of 100 mA or more are needed to sustain thruster ignition and operation. The densities of 10^{17} m^{-3} were not high enough to produce the desired current.

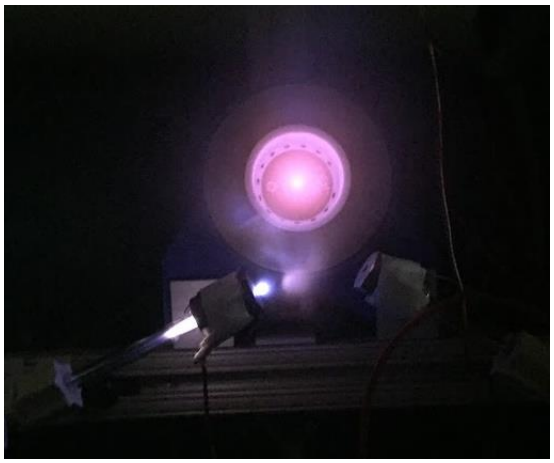

Figure 4.10. Hall thruster testing with heaterless, insertless cathode.

4.5 Optimal Operation

It was determined that the cathode could be operated at more extreme conditions to achieve the desired output. At a flow rate of 30 sccm, a pulse width of 200 ns, a frequency of 5 kHz, and a voltage of 5 kV, a stable plume was achieved that output 150 mA of current to the anode. However, with an input power of 75 W, this exceeded the low power requirements of small satellites. With that being said, after ignition of the plume the voltage could be reduced to 3 kV while maintaining the same current output of 150 mA. This

reduced the power input to a more manageable 30 W. Additionally, the flow rate could be decreased to 10 sccm, which is more suitable for small satellite operation. Unfortunately, operating at this condition caused significant electromagnetic interference. This caused damage to the surrounding equipment and caused a limit to this experiment.

With all designs, the cathode was able to ignite in less than 10 seconds. This qualifies as a fast start cathode, fulfilling one requirement of small satellite operation.

4.6 Conductive Insert Materials

Further testing was done with the addition of an insert material inside the cathode tube. Normal operation of this cathode produces high temperatures in the ion collector, estimated at 100° C+, allowing for the cathode itself to potentially serve as a heater for the insert material. Initially, 0.5 inches of molybdenum wire was coiled and inserted into the tube. This showed promise, as the plume became more stable and physically brighter than the insertless cathode. In order to further explore this design, a 1-inch length cylinder of molybdenum foil was wrapped around the inner diameter of the tube. This created an even stronger plume, and had a larger current output than the insertless design. It appeared, however, that this was caused by the increased conductive surface area and not the actual emission from the molybdenum. Molybdenum's work function is 4.37 eV which, based on the Richardson-Duschman equation, requires 3000 ^{o}C to achieve a current emission of 20 A/cm^{2}. This temperature was most likely not reached as the fused quartz tube material has a melting point of 1650 ^{o}C and no damage to the tube was observed, so it is clear that thermionic emission was not achieved.

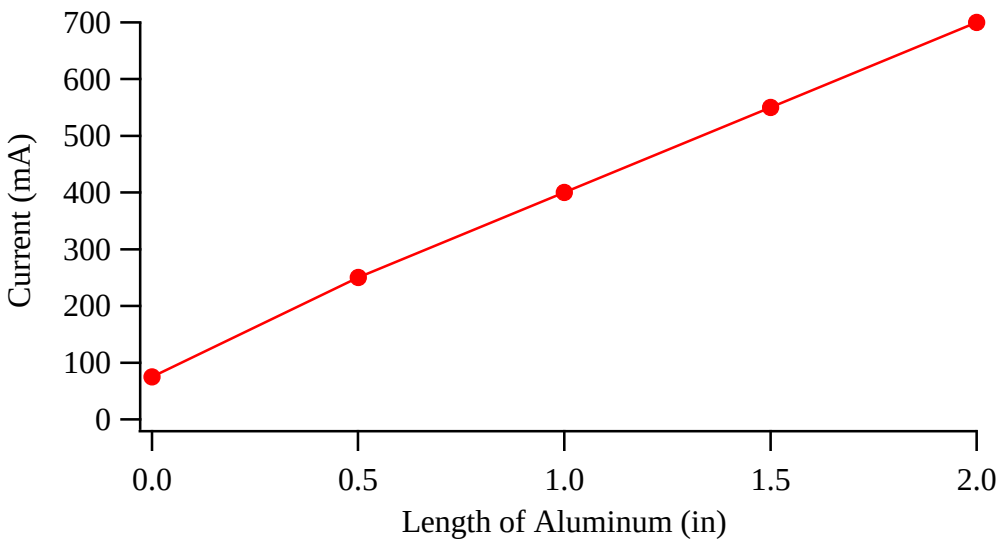

Figure 4.11. The effects of surface area on current output.

To test the effect of insert area without thermionic emission, a 1-inch long aluminum foil cylinder was used. The same results were obtained as the molybdenum, so various lengths of aluminum foil were used to test the effect of surface area on the current output. The results from these tests can be seen in Figure 4.11.

The results clearly show the increased conducting surface area from the foil increases the current. The plasma inside the tube was also visually larger and brighter. It is important to note, however, that the output plume was never stable. These brief moments of high current output were limited by heavy arcing and an oscillating plume. These currents were the average output during the highest moments of stability. These averages gave useable currents with an input power of 50 W or less.

Chapter 5

DISCUSSION

Research is to see what everybody else has seen, and to think what nobody else has thought. – Albert Szent-Gyorgyi

5.1 Cathode Performance

This work shows that it is possible to generate 150 mA of current using 30-75 W of power from a heaterless, insertless cathode in a stable mode of operation. The MPHC can be ignited in less than 10 seconds, allowing fast thruster starts. Higher currents can be achieved using any conductive insert material and thus increasing the conductive surface area. However, the insert may increase plume instability. It was shown that both stability and performance are heavily dependent on the operating characteristics. At higher voltages, pulse widths, flow rates, and frequencies, the cathode can provide higher electron densities, and therefore higher currents. However, these different conditions must be balanced with each other to provide a stable plume. Additionally, precautions must be made at the extremes of these operating conditions to prevent electronic interference and unwanted interactions with surrounding equipment. The cathode can provide suitable current to power a small EP thruster, and could be useful to small satellites. Before it can achieve this goal, however, further investigation and improvements are needed.

5.1.1 Limitations

The MPHC operated at a variety of conditions but was rarely able to produce high electron densities. It was generally found that at higher flow rates, frequencies, pulse widths, and voltages, higher densities were produced. However, at powers below the desired 10 W, the highest density was found to be 1.5 x 10^{17} m^{-3}. By assuming that the electron density in the plume is roughly equal to that inside the quartz tube, an estimation can be made of the maximum current in the quartz tube[16]. This calculation is shown in Equation 3.15.

$$\mathrm{I} = A_T q n_e \left(\frac{8kT_e}{\pi M}\right)^{\frac{1}{2}} \tag{3.15}$$

For an electron density of 1.5 x 10^{17} m^{-3}, temperature of 6.2 eV, and tube diameter of 4 mm, the current was calculated to be 11 mA. While the measured currents are around 10 mA, this approximate limit shows that a significant increase in density, temperature, or exit area is needed to improve current output to the 100's of mA levels suitable for EP thrusters. The difficultly with increasing these properties, however, is that the operational range of the MPHC with pulsed dc is limited by stability. There was a limited range of operating conditions that produced a consistently stable plume. At higher voltages, for example, the plume would oscillate between a dim, low density plume, and a bright, higher density plume, as seen in Figure 4.9. If the voltage was too high, the plume would transition into arc mode and cause damage to cathode elements.

However, the power model discussed in Equations 3.11-14 demonstrated that higher densities were possible. Specifically, using an input power of 10 W and a plasma length and radius of 10 mm and 4 mm, respectively, the theoretical electron density was found to

be 2.5 x 10^{18} m^{-3}. This density is consistent with the higher currents of 50-100 mA measured during the tests with increased plasma surface area using the conductive inserts.

Additionally, the MPHC was further limited by the electromagnetic interference (EMI) produced by the pulsed dc signal. The EMI is a signal that "leaks" through the wires connecting to the pin inside the vacuum chamber. This signal causes erroneous voltage readings and can be damaging to the turbopump that conditions the vacuum chamber. At higher voltages, the EMI intensifies. This limited the amount of time the cathode could be operated at the highest performing conditions. The EMI could be diminished with sufficient shielding of the operating cables. The high voltage pulsed dc signal needs to be transported to the pin directly by a fully shielded coaxial cable. Optimally, the cathode would have a direct port connection to a coaxial cable. This could significantly reduce the EMI and protect equipment, allowing for increased performance and prolonged operation of the cathode.

5.1.2 Cathode Improvements

Adding another electron source, such as an emissive material, could increase the electron density and therefore the current. Tests were conducted using thermionic materials such as molybdenum as an insert material. The effects of adding an insert material were expected to increase performance. However, the performance was affected in an unexpected manner. The material itself did not appear to emit electrons, but it did increase the output current. This was caused by the increased metallic surface area, which led to a larger plasma plume. The added surface area enhanced the electric field and increased ionization. This allowed for the increase in output current previously shown in Figure 4.11.

The stability of the plume still limits this method. The added ionization appears to induce arcing mode more rapidly, causing the plume to rapidly fluctuate and potentially cause damage to surrounding equipment. This method shows promise, however, and could be useful in improving this cathode.

During these tests, it was found that by decreasing pulse width and frequency, voltage could be increased. This allowed for much higher levels of stability in tests with no insert material. As discussed, the optimal condition produced 150 mA of current with input powers ranging from 30-75 W. The limiting factor of this operation was EMI. It is believed that the input power could be further reduced with more variation to the operating conditions, but the EMI limited these tests.

5.2 Comparison to Literature

As shown in Table 5.1, the MPHC produces a lower current than other designs. However, using xenon could increase the current output of the MPHC as well. As seen in the table, most cathodes operate with xenon as the propellant. Argon was chosen for the MPHC because it is a low cost gas that was more easily available. Furthermore, this design has other advantages. For example, the heaterless cathode developed by Lev, et al.[41] had significant issues with the deterioration of the cathode insert. This cathode can eliminate the need for the insert and still provide sufficient current for the propulsion needs of small satellites. Additionally, the startup time for this cathode is less than all cathodes that use an insert material. This cathode provides a novel and unique method for providing a low power, fast start neutralizing source.

Table 5.1. A summary of hollow cathode technology.

Author	Cathode Type	Propellant Gas	Discharge Current	Power	Efficiency
Polk, et al.[27]	BaO	Xenon	13 A	~200 W	15.4 W/A
Goebel, Watkins, and Jameson[58]	LaB_6	Xenon	10-100 A	125-160 W	1.6-12.5 W/A
Goebel and Chu[8]	LaB_6	Xenon	60 to 250 A	200-340 W	1.36-3.33 W/A
Hatakeyama, et al.[6]	RF	Xenon	1-2 A	80 W	40-80 W/A
Jahanbakhsh, et al.[44]	RF	Argon	0.2-0.5 A	45-85 W	170-225 W/A
Godyak, et al.[49]	RF	Xenon	0.5-5 A	200 W	4-40 W/A
Vekselman, et al.[36]	Heaterless	Xenon	0.5-1.5 A	30 W	20-60 W/A
Schatz[35]	Heaterless	Xenon	1-15 A	100 W	6.67-100 W/A
Lev, et al.[41]	Heaterless	Xenon	0.5-1 A	30-40 W	40-60 W/A
Hidaka, et al.[51]	Electron Cyclotron Resonance	Argon/Xenon	0.7 A	200 W	285.7 W/A
Rand and Williams[37]	Electride	Iodine/Xenon	15 A	50 W	3.33 W/A
Gott and Xu	Heaterless, Insertless	Argon	0.15-0.5 A	30-75 W	60-500 W/A

Chapter 6

CONCLUSION

The measure of greatness in a scientific idea is the extent to which it stimulates thought and opens up new lines of research.
– Paul Dirac

6.1 Cathode Summary

A heaterless, insertless microplasma cathode was developed that may be capable of powering a small EP thruster. The MPHC operates by ionizing argon gas in a quartz tube and separating ions and electrons. Langmuir probe measurements showed that increasing flow rate, pulse width, frequency, and voltage can increase electron density and output current. Additional testing showed that by decreasing pulse width and frequency, voltage can be further increased. This change can dramatically increase output current.

The MPHC can produce 150 mA of current and can start in less than 10 seconds, which both meet the requirements for small satellites. However, the use of 30-75 W of input power and 25-35 sccm exceeds the desired limits for power and propellant. Additionally, the MPHC is limited by plume stability and EMI. Input power, flow rate, and EMI can all be reduced, but more developments are needed to reach desired levels.

The contribution of this work to the field of electric propulsion is the addition of a cathode that broadens the possibilities for small satellite technology. The MPHC allows for the use of small Hall thrusters on small satellites due to the lower power input, fast

startup time, and efficient current output. The MPHC is small in size and built from durable materials that would make it well suited for a space environment. This could increase efficiency and decrease costs for the satellite industry and expand the utility of EP thrusters. Additionally, microplasmas were further studied and the effects of various voltage signals were documented.

6.2 Future Work

The MPHC is currently limited most significantly by EMI. The EMI signal damages equipment and prevents full testing of the optimized conditions. Work needs to be done to find a way to directly connect the powered pin of the cathode to a coaxial cable using a shielded connector. Additionally, the whole cathode will need to be shielded to prevent the signal from being broadcast through the plasma. This could be accomplished by creating a Faraday cage in which the cathode can operate.

Once the EMI is reduced, the cathode can be further improved. The current operating conditions produce the desired current with the desired startup time, but could use improvement with the input power. The flow rate, frequency, and pulse width could be adjusted further to reduce the input voltage. Additionally, further studies with tube length, plasma surface area, and propellant gas could find other methods of decreasing input power.

Langmuir probe studies could also further characterize the optimal conditions. The EMI limited the studies of the higher voltages, preventing electron temperature and density measurements. Due to visual changes and increased current output, it is believed that the electron density is much higher in tests with significantly higher voltages.

Furthermore, optical emission spectroscopy could be used to verify all measurements. This would require the development of a collisional radiative model specific to the operating conditions of this cathode. This method utilizes argon emission spectral intensities to identify plasma properties. By comparing the observed intensity ratios to the theoretical values for given conditions, the observed electron temperature and density can be found.

Finally, this cathode could be further tested with EP devices. With the output current that it presently produces, it could power small Hall thrusters. Tests with HETs and Ion thrusters could find the limits of the cathode's lifetime and current output. Overall, these tests would determine the full capabilities of this cathode.

Appendix A

Data File Directory
All files can be found in the PERL directory folders in the lab's Google Drive.

Folder	
PERL/Data Directory/Ryan/Cathode	
Subfolder	Description
Calculated Data	All calculations and plots from this work
Langmuir Probes	All raw data from Langmuir probe tests
OES	All raw data from OES Tests
Papers	All Papers used and referenced in this work
Produced Work	Papers, presentations, and posters developed from this work
Cathode Pictures	Pictures of the cathode operation and design

REFERENCES

[1] Warner, D., and Force, A., "Advanced Cathodes for Next Generation Electric Propulsion Technology," *Arc.Aiaa.Org*, 2008, p. 172.

[2] Krejci, D., and Lozano, P., "Space Propulsion Technology for Small Spacecraft," *Proceedings of the IEEE*, 2018.

[3] Blandino, J., Roy, T., Sartorreli, R., and Gamero-Costano, M., "Measurements of Plasma Potential in Colloid Thruster Plumes," *39th AIAA/ASME/SAE/ASEE Joint Propulsion Conference and Exhibit*, American Institute of Aeronautics and Astronautics, 2003.

[4] Taubin, M., Chesnokov, D., and Pavlov, A., "Cathodes for medical purpose X-Ray tubes," *Journal of Physics: Conference Series*, 2017.

[5] Goebel, D. M., Watkins, R. M., and Jameson, K. K., "LaB6 Hollow Cathodes for Ion and Hall Thrusters," *Journal of Propulsion and Power*, vol. 23, May 2007, pp. 552–558.

[6] Hatakeyama, T., Irie, M., Watanabe, H., Okutsu, A., Aoyagi, J., and Takegahara, H., "Preliminary Study on Radio Frequency Neutralizer for Ion Engine," *30th International Electric Propulsion Conference*, 2007, p. IEPC-2007-226.

[7] Levi, R., "New Dispenser Type Thermoionic Cathode," *Journal of Applied Physics*, vol. 24, 1953, p. 233.

[8] Goebel, D., Chu, E., and Jpl, "High Current Lanthanum Hexaboride Hollow Cathodes for High Power Hall Thrusters," *32nd International Electric Propulsion Conference*, 2011, pp. 1–16.

[9] Moselhy, M., Petzenhauser, I., Frank, K., and Schoenbach, K. H., "Excimer emission from microhollow cathode argon discharges," *Journal of Physics D: Applied Physics*, vol. 36, 2003, pp. 2922–2927.

[10] Xu, K. G., and Doyle, S. J., "Measurement of atmospheric pressure microplasma jet with Langmuir probes," *Journal of Vacuum Science & Technology A: Vacuum, Surfaces, and Films*, vol. 34, 2016, p. 51301.

[11] Davis, P., "Comparison of Heating Property of LaB6 and CeB6 by Back Bombardment Effect in Thermoionic RF Gun," *Journal Korean Physical Society*, 2011.

[12] Wirz, R. E., "Development of Cathode Technologies for a Miniature Ion Thruster," *39th AIAA/ASME/SAE/ASEE Joint Propulsion Conference & Exhibit*, 2003, p. AIAA 2003-4722.

[13] Tolt, Z. L., Mckenzie, C., Espinosa, R., Snyder, S., and Munson, M., "CNT cold cathodes for application in low current x-ray tubes," *Technical Digest of the 20th International Vacuum Nanoelectronics Conference, IVNC 07*, 2007, pp. 65–66.

[14] Gamero-Castaño, M., and Hruby, V., "Characterization of a Colloid Thruster Performing in the micro-Newton Range," *27th International Electric Propulsion Conference*, 2001, pp. 15–19.

[15] Cronin, J. L., "Modern Dispenser Cathodes," *IEE Proceedings I - Solid State and Electron Devices*, vol. 128, 1981, pp. 19–32.

[16] Goebel, D. M., and Katz, I., *Fundamentals of Electric Propulsion: Ion and Hall Thrusters*, John Wiley and Sons, 2008.

[17] Longmier, B. W., and Hershkowitz, N., "Electrodeless Plasma Cathode for

Neutralization of Ion Thrusters," *41st AIAA/ASME/SAE/ASEE Joint Propulsion Coference & Exhibit*, 2005, p. AIAA 2005-3856.

[18] Williams, M. D., Leung, K. N., Matuk, C. A., Wilde, S. B., Berkeley, L., Benveniste, V. M., Graf, M. A., Horsky, T. N., Saadatmand, K., Corporation, E., and Operations, S. E., "Development of an Rf Driven Plasma Cathode for Ion Sources," *Proceedings of 1997 Particle Accelerator Conference*, 1997, pp. 2767–2769.

[19] Plasek, M. L., Wordingham, C. J., and Mata, S. R., "Experimental Investigation of a Large-Diameter Cathode," *50th AIAA/ASME/SAE/ASEE Joint Propulsion Conference*, 2014.

[20] Okawa, Y., Kitamura, S., Satomi Kawamoto, Iseki, Y., Hashimoto, K., and Noda, E., "An experimental study on carbon nanotube cathodes for electrodynamic tether propulsion," *Acta Astronautica*, vol. 61, Dec. 2007, pp. 989–994.

[21] Arnold, S. S., Nuzzaci, R., and Gordon-Ross, A., "Energy budgeting for CubeSats with an integrated FPGA," *IEEE Aerospace Conference Proceedings*, 2012.

[22] Heidt, H., Puig-Suari, J., Moore, A. S., Nakasuka, S., and Twiggs, R. J., "CubeSat: A new Generation of Picosatellite for Education and Industry Low-Cost Space Experimentation," *AIAA/USU Conference on Small Satellites*, 2000, pp. 1–19.

[23] Viscio, M. A., Viola, N., Corpino, S., Stesina, F., Fineschi, S., Fumenti, F., and Circi, C., "Interplanetary CubeSats system for space weather evaluations and technology demonstration," *Acta Astronautica*, vol. 104, 2014, pp. 516–525.

[24] Dankanich, J. W., Polzin, K. a, Calvert, D., Kamhawi, H., Introduction, I., Manager, P., Development, T., Engineer, L. S., Systems, F., Division, E., and Branch, P., "The iodine Satellite (iSAT) Hall Thruster Demonstration Mission Concept and Development," *50th AIAA/ASME/SAE/ASEE Joint Propulsion Conference*, 2014, pp. 1–13.

[25] Hofer, R. R., Randolph, T. M., Oh, D. Y., Snyder, J. S., and Grys, K. H. De, "Evaluation of a 4.5 kW Commercial Hall Thruster System for NASA Science Missions," *42nd AIAA/ASME/SAE/ASEE Joint Propulsion Conference & Exhibit*, 2006, pp. 1–26.

[26] Jameson, K. K., Goebel, D. M., Hofer, R. R., and Watkins, R. M., "Cathode Coupling in Hall Thrusters," *International Electric Propulsion Conference*, 2007, pp. 1–20.

[27] Polk, J. E., Mikellides, I. G., Capece, A. M., and Katz, I., "Barium depletion in hollow cathode emitters," *Journal of Applied Physics*, vol. 119, 2016.

[28] VAN Stratum, A. J. A., VAN Os, J. G., Blatter, J. R., and Zalm, P., "Barium-aluminum-scandate dispenser cathode," 1977.

[29] Storms, E. K., and Mueller, B. a., "A study of surface stoichiometry and thermionic emission using LaB6," *Journal of Applied Physics*, vol. 50, 1979, p. 3691.

[30] Gallagher, H. E., "Poisoning of LaB6 cathodes," *Journal of Applied Physics*, vol. 40, 1969, pp. 44–51.

[31] Futamoto, M., Nakazawa, M., Usami, K., Hosoki, S., and Kawabe, U., "Thermionic emission properties of a single-crystal LaB6 cathode," *Journal of Applied Physics*, vol. 51, 1980, pp. 3869–3876.

[32] Noord, J. L. Van, Kamhawi, H., and Mcewen, H. K., "Characterization of a High

Current, Long Life Hollow Cathode," *Proceedings of the International Electric Propulsion Conference 2005 (IEPC05)*, 2005, pp. 1–12.
[33] MIRTICH, M., "Investigation of hollow cathode performance for 30-cm thrusters," *Archive Set 104*, 1963.
[34] Aston, G., "Hollow cathode startup using a microplasma discharge," *Review of Scientific Instruments*, vol. 52, Aug. 1981, pp. 1259–1260.
[35] Schatz, M. F., "Heaterless Ignition of Inert Gas Ion Thruster Hollow Cathodes," *AIAA/DGLR/JSASS 18th International Electric Propulsion Conference*, 1985, p. AIAA-85-2008.
[36] Vekselman, V., Krasik, Y., Gleizer, S., Gurovich, V., Warshavsky, A., Rabinovich, L., and Technion, "Characterization of a Heaterless Hollow Cathode," *Journal of Propulsion and Power*, vol. 29, 2013, pp. 475–486.
[37] Rand, L. P., and Williams, J. D., "Instant Start Electride Hollow Cathode," *33rd International Electric Propulsion Conference*, 2013, pp. 1–11.
[38] Rand, L. P., and Williams, J. D., "A calcium aluminate electride hollow cathode," *IEEE Transactions on Plasma Science*, vol. 43, Jan. 2015, pp. 190–194.
[39] Caruso, N. R. S., and Mcdonald, M. S., "Thermionic Emission Measurements of 12(CaO)-7(Al2O3) Electride in a Close-Spaced Diode," *Iepc2017*, vol. 12, 2017, pp. 1–10.
[40] Drobny, C., Tajmar, M., and Wirz, R. E., "Development of a C12A7 Electride Hollow Cathode," *35th International Electric Propulsion Conference*, 2017, pp. 1–8.
[41] Lev, D., Mikitchuk, D., and Appel, L., "Development of a Low Current Heaterless Hollow Cathode for Hall Thrusters," *34th International Electric Propulsion Conference*, 2015, p. IEPC-2015-163.
[42] Farnell, C. C., Williams, J. D., and Wilbur, P. J., "Characteristics of Energetic Ions Emitted from Hollow Cathodes," *28th International Electric Propulsion Conference*, 2003, p. IEPC-03-072.
[43] Jahanbakhsh, S., and Celik, M., "Experimental Study of the Effects of Different Design Parameters on the Plasma Characteristics and the Extracted Current of a Prototype Radio-Frequency," *34th International Electric Propulsion Conference*, 2015, p. IEPC-2015-108.
[44] Jahanbakhsh, S., Satir, M., and Celik, M., "Study of electron current extraction from a radio frequency plasma cathode designed as a neutralizer for ion source applications," *Review of Scientific Instruments*, vol. 87, 2016, pp. 2–7.
[45] Weis, S., Schartner, K.-H., Löb, H., and Feili, D., "Development of a capacitively coupled insert-free RF-neutralizer," *Proceedings of the International Electric Propulsion Conference 2005 (IEPC05)*, 2005, p. IEPC-2005-086.
[46] Raitses, Y., Hendryx, J. K., and Fisch, N. J., "A Parametric Study of Electron Extraction from a Low Frequency Inductively Coupled RF-Plasma Source," *31st International Electric Propulsion Conference*, 2009, p. IEPC-2009-024.
[47] Diamant, K. D., "Resonant Cavity Hollow Cathode," *41 st AIAAASMESAEASEE Joint Propulsion Conference Exhibit*, 2005, pp. 1–12.
[48] Kuninaka, H., Nishiyama, K., Shimizu, Y., and Toki, K., "Flight status of cathode-less microwave discharge ion engines onboard Hayabusa asteroid explorer," *40th AIAA/ASME/SAE/ASEE Joint Propulsion Conference & Exhibit*, vol. 52, 2004, p.

AIAA 2004-3438.
[49] Godyak, V., Raitses, Y., and Fisch, N. J., "RF plasma cathode-neutralizer for space applications," *30th International Electric Propulsion Conference*, 2007, p. IEPC-2007-266.
[50] Getty, W. D., and Geddes, J. B., "Size-scalable, 2.45-GHz electron cyclotron resonance plasma source using permanent.pdf," *Journal of Vacuum Science & Technology*, vol. 12, 1998, pp. 408–415.
[51] Hidaka, Y., Foster, J. E., Getty, W. D., Gilgenbach, R. M., and Lau, Y. Y., "Performance and analysis of an electron cyclotron resonance plasma cathode," *Journal of Vacuum Science & Technology A*, vol. 25, 2007, pp. 781–790.
[52] Weatherford, B. R., Foster, J. E., and Kamhawi, H., "Electron current extraction from a permanent magnet waveguide plasma cathode," *Review of Scientific Instruments*, vol. 82, Sep. 2011.
[53] Plasek, M., Jorns, B., Choueiri, E., and Polk, J., "Exploration of RF-Controlled High Current Density Hollow Cathode Concepts," *48th AIAA/ASME/SAE/ASEE Joint Propulsion Conference & Exhibit*, American Institute of Aeronautics and Astronautics, 2012.
[54] Plasek, M. L., Wordingham, C., and Choueiri, E., "Modeling and Development of the RF-Controlled Hollow Cathode Concept," *49th AIAA/ASME/SAE/ASEE Joint Propulsion Conference*, American Institute of Aeronautics and Astronautics, 2013.
[55] Plasek, M. L., Wordingham, C. J., and Choueiri, E. Y., "Resonant Mode Transition in the RF-Controlled Hollow Cathode," *33rd International Electric Propulsion Conference*, 2013, pp. 4–11.
[56] Chen, F., *Plasma Diagnostic Techniques*, New York: Academic Press Inc., 1965.
[57] Liebermann, A. M., and Allan, L. J., *Plasma Discharges and Material Processing*, 2005.
[58] Goebel, D. M., Jameson, K. K., Watkins, R. M., Katz, I., and Mikellides, I. G., "Hollow cathode theory and experiment. I. Plasma characterization using fast miniature scanning probes," *Journal of Applied Physics*, vol. 98, 2005.